NASA TECHNICAL NOTE

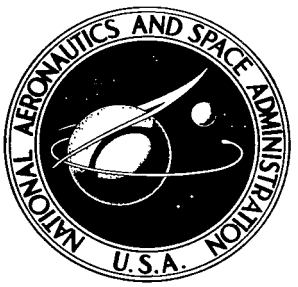

NASA TN D-8454

EXPERIMENTAL INVESTIGATION OF A SWEPT-STRUT FUEL-INJECTOR CONCEPT FOR SCRAMJET APPLICATION

Griffin Y. Anderson, Patricia G. Reagon, Paul B. Gooderum, and W. Roger Russin

Langley Research Center
Hampton, Va. 23665

NATIONAL AERONAUTICS AND SPACE ADMINISTRATION • WASHINGTON D. C. • AUGUST 1977

1. Report No.	2. Government Accession No.	
NASA TN D-8454		

4. Title and Subtitle
EXPERIMENTAL INVESTIGATION OF A SWEPT-STRUT FUEL-INJECTOR CONCEPT FOR SCRAMJET APPLICATION

5. Report Date
August 1977

6. Performing Organization Code

7. Author(s)
Griffin Y. Anderson, Patricia G. Reagon, Paul B. Gooderum, and W. Roger Russin

8. Performing Organization Report No.
L-11050

10. Work Unit No.
505-05-41-01

9. Performing Organization Name and Address
NASA Langley Research Center
Hampton, VA 23665

11. Contract or Grant No.

13. Type of Report and Period Covered
Technical Note

12. Sponsoring Agency Name and Address
National Aeronautics and Space Administration
Washington, DC 20546

14. Sponsoring Agency Code

15. Supplementary Notes

16. Abstract

Results are presented of an experiment to investigate the behavior at Mach 4 flight conditions of the swept-strut fuel-injector concept employed in the Langley integrated modular scramjet engine design. Autoignition of the hydrogen fuel was not achieved at stagnation temperatures corresponding to a flight Mach number of 4; however, once ignition was achieved, stable combustion was maintained. Pressure disturbances upstream of the injector location, which were caused by fuel injection and combustion, were generally not observed; this indicates the absence of serious adverse combustor-inlet interactions. Mixing performance and reaction performance determined from probe surveys and wall pressure data indicate that high combustion efficiency should be obtained with the combustor length provided in the scramjet engine design. No adverse interaction between the perpendicular and parallel fuel-injection modes was observed.

17. Key Words (Suggested by Author(s))
Scramjet
Hypersonic propulsion
Hydrogen
Fuel injection
Combustion efficiency

18. Distribution Statement
Unclassified - Unlimited

Subject Category 07

19. Security Classif. (of this report)	20. Security Classif. (of this page)	21. No. of Pages	22. Price*
Unclassified	Unclassified	63	$4.50

* For sale by the National Technical Information Service, Springfield, Virginia 22161

EXPERIMENTAL INVESTIGATION OF A SWEPT-STRUT FUEL-INJECTOR CONCEPT FOR SCRAMJET APPLICATION

Griffin Y. Anderson, Patricia G. Reagon,
Paul B. Gooderum, and W. Roger Russin
Langley Research Center

SUMMARY

Results are presented of an experiment to investigate the behavior at Mach 4 flight conditions of the swept-strut fuel-injector concept employed in the Langley integrated modular scramjet engine design. Autoignition of the hydrogen fuel was not achieved at stagnation temperatures corresponding to a flight Mach number of 4; however, once ignition was achieved, stable combustion was maintained. Pressure disturbances upstream of the injector location, which were caused by fuel injection and combustion, were generally not observed; this indicates the absence of serious adverse combustor-inlet interactions. Mixing performance and reaction performance determined from probe surveys and wall pressure data indicate that high combustion efficiency should be obtained with the combustor length provided in the scramjet engine design. No adverse interaction between the perpendicular and parallel fuel-injection modes was observed.

INTRODUCTION

The NASA Langley Research Center is actively engaged in a program to evolve new concepts for airframe integrated scramjet engines. Reference 1 presents a discussion of general design considerations for integrated engines and describes a particular modular scramjet concept which employs swept inlet compression surfaces to achieve good performance potential for a broad range of flight speed with fixed geometry. The upper part of figure 1 shows an integrated engine vehicle system and a photograph of a model of two adjacent modules of the scramjet engine concept; the sidewall of the nearer module is removed to show the fuel-injection struts, and the engine components - inlet, combustor, and nozzle - are identified. Extensive aerodynamic tests of the inlet concept for this modular scramjet design have been conducted and provide detailed data on the inlet mass capture, aerodynamic compression, and pressure recovery characteristics. (See ref. 2.) These data substantiate the favorable performance potential of the inlet concept and provide a basis for detailed design considerations for the combustor.

The approach adopted for fuel-injector and combustor design is described in references 1 and 3. The sketch in the lower part of figure 1 shows a cross section through the fuel-injection struts in a plane parallel to the engine cowl. As indicated by the arrows, fuel is introduced perpendicular to the inlet air flow from orifices located downstream of small rearward facing steps at the inlet throat and parallel to the flow from orifices on the trailing edges of the struts. The purpose of the steps is to isolate the forward (compression) sur-

faces of the struts from the fuel injection and the combustion generated pressure rise. At high flight speeds (Mach 7 and above) where thermal choking of the combustor is not a problem, all fuel is injected from the perpendicular injectors to achieve the most rapid possible mixing and combustion for best performance. At lower speeds (Mach 5 to Mach 7) a combination of perpendicular and parallel injection is used to stretch out the heat release over the entire length of the combustor. This combination of perpendicular and parallel injection avoids thermal choking of the combustor and inlet unstart which would be likely to occur at these speeds with all perpendicular injection. In this fixed geometry design, tailoring heat release distribution alone is not sufficient to avoid thermal choking at speeds below Mach 5. Either fuel flow for the combustor must be reduced below stoichiometric (with an attendant reduction in engine thrust) or some supersonic-subsonic-supersonic mode, in effect a "transonic" mode, of combustion must be adopted. Although this latter solution is of particular interest to the engine designer, analytical means are not available for describing such transonic mixing-reacting flows in a realistic manner; also, ignition, stability, and performance characteristics are difficult to estimate, a priori.

There exists another potential problem which is related to the particular design approach for the module inlet. As a result of sweep, the inlet compression waves between the struts become detached at flight Mach numbers below about 5. The inlet flow at the throat becomes three dimensional, and flow conditions vary with position along the strut shoulder from the underside of the vehicle to the engine cowl. Of course, when waves in the throat region are detached, pressure disturbances in the combustor may directly influence the inlet flow. For example, if waves in the inlet throat region are detached, a combustion pressure rise from perpendicular injection near the top of the module (adjacent to the underside of the vehicle) would produce compressions that would lie ahead of the strut shoulder (because detached waves propagate at an angle steeper than the sweep angle) and affect the inlet flow field in the cowl region. Thus, the use of sweep in the design of the inlet compression flow field provides the potential for adverse inlet-combustor interaction at low speeds where waves in the inlet become detached. This potential interaction and the three-dimensional nature of the inlet flow field, coupled with the need for high-thrust "transonic" combustion, make accurate experimental simulation of the fuel injection region of the engine module an important objective in concept development.

The purpose of this paper is to describe results from an experiment designed to investigate this swept-strut fuel-injection concept at Mach 4 flight conditions by simulating a segment of the flow around the center strut. (See fig. 1.)

In order to reduce the size and complexity of the hardware required for a complete-inlet-combustor experiment, a direct-connect approach (i.e., combustor entrance conditions created by a specially designed nozzle) was chosen for the swept-strut fuel-injection experiment. The nonuniform flow at the inlet throat in the engine (produced by detached swept compressions created by the inlet geometry) is approximated by a two-dimensional flow which is essentially uniform along the swept step and fuel-injection location. Three-dimensional effects exist in the engine as a result of the vehicle boundary layer and detached waves in the inlet compression process but are not simulated in this

experiment; however, the potential for inlet-combustor interaction is provided by selecting the step sweep angle and approach-flow Mach number such that the component of Mach number perpendicular to the step is near the sonic velocity attained in the engine. The principal questions addressed by the experiment are:

1. Will autoignition occur at Mach 4 flight conditions and will stable combustion be maintained?

2. Will pressure disturbances, due to fuel injection and combustion, arise and propagate upstream of the step, thus indicating an adverse combustor-inlet interaction?

3. What mixing and reaction performance will be achieved for stoichiometric injection with a nominal fuel split of 30-percent perpendicular injection and 70-percent parallel injection? Also, does any adverse interaction occur between perpendicular injection and parallel injection?

SYMBOLS

C_f friction coefficient

E_r local reaction parameter (degree to which chemical equilibrium is achieved at a point in the flow)

F stream thrust

f ratio of burner fuel flow to oxidizer flow, $\frac{\text{Burner fuel flow}}{\text{Air flow + Oxygen flow}}$

H total enthalpy

h total flow width at step, 2.74 cm (see fig. 3)

I burner free oxygen parameter, $\frac{\text{Oxygen flow (0.0823)}}{\text{Burner fuel flow}}$; for I = 1.0 test gas has same oxygen content as air

K combustor integral factor (integral of combustor wall pressure force divided by the product of difference between combustor exit area and entrance area and the average of combustor entrance pressure and exit pressure)

M Mach number

p pressure

Q duct heat

T temperature

w	mass flow
x	axial location measured from step
z	dimensionless survey probe location (see fig. 8)
η_c	overall combustion efficiency (fraction of injected fuel reacted)
η_m	overall mixing efficiency (fraction of injected fuel mixed so that it can react)
$\bar{\phi}$	mass average equivalence ratio

Subscripts:

h	burner
j	injected fuel
t	stagnation

APPARATUS AND PROCEDURE

The swept-strut fuel-injector model with one sidewall removed is shown in perspective view in figure 2; dimensions and other details are shown in figure 3. The model consists of two vertical-plane sidewalls (which represent bounding stream surfaces for the flow fueled by the center strut in the engine design) and a contoured centerbody (symmetric about its vertical midplane like the engine) which provide supersonic flow simulating combustor entrance conditions and appropriate locations for fuel-injection ports. Identical choked throats are produced by the contour on both sides of the model centerbody in a plane perpendicular to the sidewalls and the entering flow direction. A supersonic nozzle contour follows each throat and is designed by the method of reference 4 to produce uniform flow parallel to the centerplane of the model. After initial tests with a Mach 1.7 nozzle contour, the centerbody was reshaped to a contour designed to produce Mach 1.3 flow. Values of Mach 1.7 and Mach 1.3 were selected to provide attached and detached waves, respectively, along the perpendicular fuel-injector location which is swept at 45° to the entering flow direction. Test gas is supplied to the model by a hydrogen-oxygen-air burner (see ref. 5) at a nominal stagnation temperature of 1000 K and a stagnation pressure of 0.8 MPa (these values simulate Mach 4 flight speed at an 18 000-m altitude). Test-gas composition is approximately 0.2095 oxygen, 0.6870 nitrogen, and 0.1035 water vapor by volume with flow rates of 3.5 kg/sec for the Mach 1.7 nozzle contour and 4.2 kg/sec for the Mach 1.3 nozzle contour.

Steps are located in a plane perpendicular to the sidewalls but swept at 45° to the entering flow direction. Choked perpendicular injectors are located downstream of the steps with four 0.2-cm-diameter holes on each side of the centerbody equally spaced 4.25 cm apart across the duct height. Three supersonic parallel injectors are located on the trailing edge of the centerbody at locations half way between the perpendicular injectors. The perpendicular and paral-

lel injectors are supplied with hydrogen from separate manifolds which can be controlled independently. An electric resistance heater is available to heat the hydrogen supplied to the perpendicular injection manifold to a stagnation temperature of about 450 K. The injector holes are sized so that, with equal fuel temperature and pressure, approximately 30 percent of the total fuel goes to the perpendicular injectors and 70 percent goes to the parallel injectors. For the Mach 1.7 nozzle contour, a fuel stagnation pressure p_t of 2.6 MPa is required for stoichiometric injection of ambient-temperature hydrogen; for the Mach 1.3 nozzle contour, p_t = 3.1 MPa is required. The corresponding ratio of jet dynamic pressure to free-stream dynamic pressure for the perpendicular injectors is approximately 3.0 for both nozzle contours.

The fuel-injector section is machined entirely from mild steel. Material thickness is generally 4 cm, or more, to provide heat sink for cooling. Pressure taps are located on the sidewall surfaces and along the bounding end planes of the centerbody, as shown in figure 4. The fuel-injector section ends in a plane perpendicular to the duct walls and joins a diverging combustor duct, as indicated in figure 3. This water-cooled combustor duct is a section of the combustor model described in reference 6. Pressure taps are located along the center lines of the diverging walls of the duct. A nine-probe pitot-pressure and gas-sample rake is located at the exit of the combustor duct. The probes span the 17-cm dimension of the duct in a plane parallel to the centerbody plane of symmetry and are equally spaced.

A typical test-run sequence is conducted in the following manner. Coolant flows are initiated; and various supply pressures for air, hydrogen, and oxygen to the test-gas burner and hydrogen fuel for the injectors are established at preselected values. With air flowing, an ignition source (hydrogen-oxygen torch) is established in the test-gas burner, and an automatic run-timer sequence is initiated, thus bringing the test-gas burner to operating conditions. Fuel flows to the perpendicular and parallel injectors start at preset times after the test-gas burner is operating. The test-gas-burner firing is generally set for 20 sec, with fuel supplied to the injectors for a duration of approximately 15 sec. Pressures are measured by strain-gage pressure transducers; wall and coolant temperatures are measured by chromel-alumel and copper-constantan thermocouples. Scanning valves are used to acquire wall-pressure values from multiple locations with a single transducer. Data recording and sequencing for the pressure scanning valves are handled by a computer-controlled digital data acquisition system. Overall measurement accuracy is generally within ±3 percent. The probe rake is positioned to a preselected point in the flow by an electromechanical actuator. The probe insertion and operation of sample valves are timed manually to collect gas samples during the fuel-injection period. Details of the probe operation, sample collection, and gas-sample analysis techniques are given in the appendix.

RESULTS AND DISCUSSION

Ignition and Flame Holding

Autoignition of the injected hydrogen fuel did not occur with a test-gas stagnation temperature of 1000 K. Various perpendicular and parallel injection

pressures and combinations were tried, but all failed to cause autoignition or to establish stable combustion inside the model. These injection conditions included (1) varying injector flow rates from 0.3 to 1.5 times the nominal value, (2) providing an initial overpressure on injection to achieve a larger disturbance than the steady injection level, and (3) exploring all combinations and sequences of initiating the perpendicular and parallel injection flows. Some burning was achieved in the boundary region of the free jet external to the model, particularly for the higher fuel flows, but combustion near the fuel-injection location did not occur.

Tests were then conducted with progressively higher stagnation temperature until autoignition and stable combustion inside the model were achieved. In these tests, either perpendicular injection, parallel injection, or injection in combination with various flow rates was used. Apparently, once ignition at the perpendicular injectors is achieved, fuel injected from the parallel injectors ignites quite readily. Ignition at the perpendicular injection location appears to be insensitive to fuel flow rate and fuel flow transients. Data on the minimum test-gas stagnation temperature for autoignition of fuel injected from the perpendicular injectors are given in table I. From this table, it is seen that autoignition temperature did not change for burner stagnation pressure between 0.5 and 0.8 MPa for the Mach 1.7 nozzle contour. A slight reduction in autoignition temperature occurred in changing from the Mach 1.7 nozzle contour to the Mach 1.3 nozzle contour; heating the hydrogen supplied to the perpendicular injector by a temperature increase of 135 K (from 300 K to 435 K) produced a reduction of 170 K in the test-gas stagnation temperature required for autoignition.

As a consequence of the preceding results, ignitors will be required for the scramjet engine module at flight speeds below about Mach 5. However, once stable combustion was achieved at the perpendicular injection location, it was found that the test-gas stagnation temperature could be reduced to 1000 K (by reducing hydrogen flow to the test-gas burner) and stable combustion would continue; that is, once ignition was achieved, the combination of model geometry (step) and perpendicular-injection disturbance provided adequate flame holding to maintain combustion at conditions simulating Mach 4 flight. For the present experiments, a test-gas-burner operating procedure was established to provide an initial stagnation temperature of about 1250 K for several seconds, followed by a rapid (1 to 2 sec) reduction of temperature to 1000 K. Perpendicular and parallel fuel-injection flows to the model were initiated immediately after ignition of the test-gas burner while the stagnation temperature was high enough to achieve autoignition and stable combustion of fuel injected to the model. Data were acquired later in the test after the stagnation temperature had been stabilized at 1000 K. This ignition procedure was used successfully to obtain all the data presented in the remainder of this report.

Wall Pressure Contours

In order to obtain an insight into the meaning of the measured wall pressure data in the injector region, isobar contour plots of the static pressures within the fuel-injector section of the model were prepared with a spline-under-tension interpolation procedure and computer-plotting routine. (See ref. 7.)

Since no significant difference was found between data at the same location on opposite sidewalls of the duct, data from both sidewalls were used to prepare the contour plots. Uniform pressure was assumed from top to bottom of the duct at the end of the nozzle contour, and a linear variation was used between the measured values of pressure at the top and the bottom of the injector-section exit. Locations of measured pressure data from which the contours were interpolated are shown in figure 4. Isobar contour plots of wall static pressure divided by burner stagnation pressure $p/p_{t,h}$ are shown in figure 5 for the Mach 1.7 nozzle contour.

Figure 5(a) shows isobars for the Mach 1.7 nozzle contour with no fuel injection. Local high and low values found by the interpolation procedure are indicated in the plot by the letters "H" and "L," respectively. The nozzle exit corresponds to the left-hand boundary of the plot where the pressure is taken as 0.225 times the burner stagnation pressure. The swept step, trailing edge, and perpendicular fuel-injector locations are also indicated. Note that the isobars in the region of the step appear relatively straight and are parallel to the step. Some end effects near the top and bottom boundaries of the figure are evident. In particular, a high pressure region is apparent on the top boundary between the step and trailing edge, and a very low pressure region exists near the bottom boundary on the trailing edge. A small region on the bottom boundary ahead of the step shows a premature drop in pressure, probably because of the boundary layer in the corner.

Figure 5(b) presents isobars with fuel injected only from the perpendicular injectors located downstream of the step at an equivalence ratio of 0.43. Pressure data from taps upstream of the step are not affected by perpendicular injection; as a result, the isobar pattern upstream of the step in figure 5(b) is very similar to the pattern without injection in figure 5(a). Downstream of the step, some differences are noted, particularly a slight increase in pressure downstream of the two perpendicular injectors nearest to the lower boundary of the plot. However, the most apparent feature is a lack of any striking change due to perpendicular fuel injection by itself, and the existence of a prominent end effect on the top boundary between the step and the trailing edge. In the lower half of figure 5(b), isobars downstream of the step appear to lie mainly parallel to the step, but near the top boundary of figure 5(b), the isobars appear to close and indicate regions of high pressure.

Figure 5(c) shows isobars for stoichiometric fuel injection with 30 percent of the fuel from the perpendicular injectors and 70 percent of the fuel from the parallel injectors located on the trailing edge of the strut. High pressure downstream of each perpendicular injector is more pronounced than in figure 5(b), resulting in the appearance of local low pressure values between injectors. In the lower half of figure 5(c), the pressure falls to these lows, rises rapidly with isobars parallel to the step, and reaches a level which is relatively uniform in the region downstream of the trailing edge. In the upper half of the figure, this pressure rise is delayed and occurs with isobars roughly perpendicular to the upper boundary between the step and the trailing edge. Also, a region of very high pressure occurs near the top boundary between the trailing edge and the exit of the model. It is interesting to note that this difference in pressure pattern between the lower and upper boundaries found with stoichiometric injection, although more pronounced, is qualitatively simi-

lar to the difference between the lower and upper boundaries with perpendicular injection only and with no injection. Again pressure data upstream of the step are not affected by fuel injection and combustion so that the pressure patterns ahead of the step in figures 5(a) to 5(c) are very similar. Thus, the injection and combustion generated pressure rise does not produce pressure disturbances which propagate upstream of the sweep direction for the Mach 1.7 nozzle contour; but there is evidence of significant end effects between the step and the trailing edge of the centerbody, particularly along the upper boundary in figure 5.

Observation of the visible flame pattern at the exit of the swept-strut injector section (with the combustor duct removed) led to speculation that less intense combustion might be occurring in the flow near the upper boundary of figure 5. This speculation was reinforced by the heating pattern observed on the injector centerbody when the model was disassembled after completion of the Mach 1.7 tests prior to remachining the nozzle contour for the Mach 1.3 tests. A photograph of this heating pattern is shown in figure 6 with the same orientation as in figure 5. The bright areas to the right of the step indicate portions of the model that reached the highest temperature. In the lower half of figure 6, the upstream edge of this heating pattern follows a line roughly parallel to the step. In the upper half of figure 6, this heating pattern is farther downstream from the step and lies nearly perpendicular to the top boundary. This behavior is similar to the isobar contours downstream of the step in figure 5(c) where rapid pressure rise begins (e.g., the 0.2 isobar in fig. 5(c) to the right of the perpendicular fuel injectors). The heating pattern in figure 6 suggests that the pressure patterns in figure 5(c) may be due to delayed ignition near the top boundary.

Since the hydrogen fuel enters the model at the top boundary and is heated as it flows toward injection ports near the bottom boundary, the difference in ignition distance might be due to a difference in fuel temperature. A thermocouple located in the perpendicular fuel injection manifold near the bottom boundary of figure 5 indicated a 450 K temperature near the end of runs with stoichiometric injection. In order to investigate fuel-temperature effects on ignition and wall pressure patterns, the Mach 1.3 nozzle contour was tested both with ambient-temperature hydrogen and with 450 K heated hydrogen supplied to the perpendicular injectors. Discussions of results with heated fuel are included with the ambient-temperature results in the remainder of this report.

Figures 7(a) to 7(d) present isobar plots for the Mach 1.3 nozzle contour with no fuel, perpendicular injection only, stoichiometric injection, and stoichiometric injection with heated fuel at 450 K supplied to the perpendicular injectors. Note that unlike the isobars in figure 5(a), the isobars near the step in figure 7(a) lie at a smaller sweep angle to the initial flow direction than does the step. Although the nozzle exit pressure is higher (0.42 times burner supply pressure), the general features of the isobar plots in figures 7(a) to 7(c) are similar to the Mach 1.7 plots in figure 5 for the same level of fuel injection. In particular, the end effect near the top boundary between the step and the trailing edge is quite prominent in figures 7(a) and 7(b). In figure 7(c), unlike figure 5(c), isobars near the trailing edge appear parallel to the sweep direction, but a region of high pressure still occurs near the top boundary between the step and the trailing edge. In figures 7(b) and 7(c), regions of low pressure appear in line with the perpendicular injectors

rather than in between, as in figure 5(c). Also, as expected for this lower Mach number (1.3), a slight indication of pressure disturbance ahead of the step is visible in figures 7(a) to 7(c). However, the dominant feature of the isobar plots (i.e., a difference in behavior between the step and the trailing edge of the centerbody on the top and bottom boundary) is unchanged. It is interesting to note that the heating pattern visible on the injector centerbody after completion of the Mach 1.3 tests with ambient-temperature fuel appeared very similar to that shown in figure 6 for the Mach 1.7 tests.

The isobar plot in figure 7(d), for 1.09 times stoichiometric injection with the temperature of the fuel supplied to the perpendicular injectors increased from 300 K to 450 K, shows considerably more disturbance in the flow ahead of the step. Pressure from the assumed undisturbed nozzle exit value of 0.42 times the burner pressure rises to about 0.48 times the burner pressure at the step location. Downstream of the step the pressure level is considerably higher than at the same location in figure 7(c) with ambient-temperature fuel supplied to the perpendicular injectors. Apparently, the fuel from the perpendicular injectors reacts more rapidly when heated to 450 K. This increased reaction produces a pressure rise and waves near the top surface which propagate ahead of the step because of the low initial Mach number. Although this disturbance of the flow ahead of the step is not desirable in the engine, more rapid reaction does tend to reduce the end effect evident on the top surface between the step and the trailing edge in figure 5 and in figures 7(a) to 7(c). Further insight into these results is available from the exit-plane-survey results discussed in the next section.

Exit-Plane Surveys

Probe surveys at the exit plane of the combustor duct ($x/h \approx 29$) made to determine the levels of mixing and combustion of the injected fuel achieved were a major goal of this experiment. The exit-plane geometry and probe orientation are shown in figure 8. The data obtained (local values of fuel mass fraction, reaction efficiency, and pitot pressure for several probe-rake positions in the exit plane) are analyzed by the techniques described in the appendix in order to develop contour plots of the measured data and other computed flow variables across the exit of the combustor. Integrated values of the test-gas and injected-fuel flow rates are calculated and are compared directly with the flows supplied to the apparatus. In addition, parameters such as exit stream thrust and mixing efficiency are calculated and are used as an overall performance index for the fuel injector and combustor design. This section presents probe survey results for stoichiometric injection with a nominal fuel split of 30-percent perpendicular injection and 70-percent parallel injection for the Mach 1.7 nozzle contour and the Mach 1.3 nozzle contour and includes results for the Mach 1.3 nozzle contour with heated fuel at 450 K supplied to the perpendicular injectors.

Contour plots.- In figures 9, 10, and 11, contour plots for the combustor duct exit plane represent the distributions of fuel, reaction, pitot pressure, mass flux, Mach number, and stagnation temperature for the Mach 1.7 tests, the Mach 1.3 tests, and the Mach 1.3 heated-fuel tests. Measured burner operating conditions for the runs used in preparing the contour plots are given in

table II. In each plot the fuel-injection orifices are located as indicated in figure 8.

The injected-fuel distribution in the exit plane of the combustor duct with the Mach 1.7 nozzle contour is shown in figure 9(a). The curves indicate contours of constant concentration. The value adjacent to each contour gives the local equivalence ratio which each contour represents. Equivalence ratio is defined as the local fuel mass fraction divided by the stoichiometric fuel mass fraction. Values of equivalence ratio greater than 1.0 indicate rich areas with excess fuel, and values less than 1.0 indicate lean areas with excess oxygen. The nearly circular contours near the bottom of figure 9(a) indicate a fuel concentration peak corresponding roughly to the location of the lowest parallel injector indicated in figure 8. Moving up from this peak, the contours show a distinct change in character. No fuel peaks corresponding to the other two parallel injectors are observed, and the fuel contours change from circular curves to roughly horizontal curves. Also, fuel concentration decreases sharply, and approximately one-third of the duct-exit plane adjacent to the top boundary has less than stoichiometric fuel concentration. Since the overall injected equivalence ratio is stoichiometric, the lean top portion indicates uneven fuel (or test-gas) distribution from top to bottom in figure 9(a). (This will be examined in more detail in a later section.) Note also that all four corners of the duct exit appear quite lean. This result is probably due to dilution of the samples taken near the corners by air entrained because of overexpansion of the combustor duct-exit flow.

The distribution of reaction in the combustor duct-exit plane is shown in figure 9(b). The local reaction parameter presented in figure 9(b) is the fraction of the least available reactant consumed (fuel in regions with fuel concentration less than stoichiometric and oxidizer in regions greater than stoichiometric) and represents the degree to which chemical equilibrium is achieved. Generally speaking, the reaction parameter is quite high; only small regions of the flow near the stoichiometric fuel-concentration contour (shown by the dashed curve in fig. 9(b)) have a reaction parameter less than 0.98. Since the sample acquisition sequence used in these tests probably did not quench reaction in the gas entering the probe, incomplete reaction in the sample most likely results from time variation in composition at the probe tip. Such fluctuations in composition give rise to alternately lean and rich combustion products entering the probe at different times (often termed "unmixedness") in regions where the mean concentration is near stoichiometric.

The pitot-pressure distribution in the exit plane is shown in figure 9(c). Most of the flow has a pitot pressure in the range from 0.21 to 0.23 times the burner supply pressure. A region of somewhat higher pitot pressure exists near the top boundary of the flow. Figures 9(a) to 9(c) represent the independent parameters measured across the combustor duct exit plane for the Mach 1.7 nozzle contour. Other flow properties are calculated by the method described in the appendix. Figures 9(d) to 9(f) show distributions of mass flux, Mach number, and stagnation temperature which are useful in understanding the details of the exit plane flow. The mass-flux distribution in figure 9(d) is relatively uniform in the bottom part of the exit plane, but high mass-flux areas are shown near the top and in the corners of the exit plane. In figure 9(e), the Mach number is on the order of 1.5 over most of the exit plane, with a slab of somewhat

higher Mach number next to the top boundary. In figure 9(f), stagnation temperature is relatively uniform at about 2.5 times the burner stagnation temperature in the portion of the flow at stoichiometric or greater equivalence ratio. (See fig. 9(a).) A slightly cooler region within the nearly circular contour labeled 2.5 exists and corresponds to the fuel peak noted in figure 9(a). Temperature decreases rapidly near the top boundary and in the corners of the exit plane.

For the Mach 1.3 nozzle contour, figures 10(a) to 10(f) show distributions of fuel, reaction, pitot pressure, mass flux, Mach number, and stagnation temperature. Generally speaking, each distribution is quite similar to the corresponding distribution shown in figures 9(a) to 9(f) for the Mach 1.7 nozzle contour. The outstanding feature in both figure 9 and figure 10 is the end-effect region of lean, cold, and high mass flux near the top of the flow.

Figures 11(a) to 11(f) show property distribution for the Mach 1.3 nozzle contour with stoichiometric injection and heated fuel at 450 K supplied to the perpendicular injectors. In figure 11(a) the maximum fuel concentration is smaller than the maximum in either figure 9(a) or figure 10(a). Note that only three surveys were available for the heated-fuel condition, compared with six for each ambient-fuel condition, so that symmetry about the midplane of the injector centerbody was assumed in constructing figure 11. Also, the concentration contours generally lie parallel to the sidewalls of the exit plane; no distinct peak corresponding to a single parallel fuel injector is apparent in figure 11, unlike figures 9(a) and 10(a). Although it is much less prominent, a fuel lean region still appears adjacent to the top boundary. Pitot pressure, mass flux, Mach number, and stagnation temperature also show in figures 11(c) to 11(f) a distinct flow region adjacent to the top boundary similar to the flow region in figures 9 and 10. Although the size of this end-effect region is smaller with heated fuel, the end effect is still the most prominent feature of the exit plane flow.

Integrations.- Contour plots show qualitative features of the exit plane flow but do not provide quantitative information in a form which can be easily adapted for direct comparison between the different nozzle contours and fuel temperatures. Of course, flow properties are defined across the entire exit plane, and appropriate integrations of various parameters can be made to allow quantitative comparison. Since figures 9 to 11 show an apparent maldistribution of fuel and test gas from top to bottom in the combustor exit plane, strip integrations of fuel and test gas in both the horizontal and vertical directions were calculated. The strips are oriented as shown in figure 8; and the results, nondimensionalized by the amount of fuel (or test gas) that would be found in each strip if the exit plane flow were uniform, are plotted in figure 12.

Figures 12(a) and 12(b) present the horizontal distributions of fuel and test gas from integration of strips parallel to the midplane of the injector centerbody. As expected from the contour plots, both fuel and test-gas distributions for the ambient-fuel-temperature tests are very nearly symmetric about the midplane. In order to construct the contour plots shown in figure 11, the heated-fuel test data were assumed symmetric. There is somewhat more fuel near the midplane of the centerbody because the three parallel injectors that provide 70 percent of the fuel are located there. The test-gas distribution in figure 12(b) shows the inverse effect, and there is no large difference in the

horizontal distribution of either fuel or test gas between the Mach 1.7 nozzle contour and the Mach 1.3 nozzle contour. Figures 12(c) and 12(d) present the vertical distributions of fuel and test gas for integration of strips perpendicular to the midplane of the injector centerbody. Again, there is somewhat more fuel near the center of the duct, but the top of the flow has somewhat less fuel than average. Test-gas distribution in figure 12(d) is more striking; the top 20 percent of the exit plane contains up to 60 percent more test gas than average. Again no large difference between the Mach 1.7 nozzle contour and the Mach 1.3 nozzle contour is apparent. The distributions with heated fuel at 450 K supplied to the perpendicular injectors show slightly more uniformity than either result with ambient temperature fuel.

A good estimate of the test-gas flow distortion found in the exit plane of the combustor duct with stoichiometric injection can be obtained from theoretical calculations of the flow in the injector section without fuel injection. Calculations were made with a three-dimensional flow-field code developed by Manuel D. Salas which uses numerical techniques similar to those applied to develop the two-dimensional code described in reference 8. The discrete step in the injector centerbody is approximated by a 6° change in wall slope at the step location. Thus, the centerbody cross section is taken as a simple swept wedge with 6° half-angle for the calculation. Theoretical isobars for the Mach 1.7 nozzle contour and the Mach 1.3 nozzle contour are shown in figures 13(a) and 13(b). Comparison with corresponding data presented in figures 5(a) and 7(a) shows good agreement. The flow behind the nozzle contour expands across the step line and continues expanding toward the trailing edge of the centerbody. Note that in figure 13(b) the swept expansion for the Mach 1.3 nozzle contour propagates ahead of the sweep line, as expected. For both Mach numbers, sweep of the expansion causes the flow to turn away from the sweep direction toward the top boundary of the flow. This turn generates compressions which propagate back along the sweep direction and cause the end effect noted on the top of the flow between the step and the trailing edge in figures 5(a) and 7(a). The net result is to increase the mass flux in the top portion of the flow.

In figures 13(c) and 13(d), the measured test-gas flow distributions at the combustor exit plane for the Mach 1.7 nozzle contour and the Mach 1.3 nozzle contour with stoichiometric injection (taken from fig. 12(d)) are compared with the calculated test-gas flow distributions without injection. The calculated distributions were obtained for planes parallel to the duct exit plane at a location near the intersection of the trailing edge of the centerbody and the top surface of the duct, as indicated by the arrows in figures 13(a) and 13(b). This location was chosen to correspond roughly to the location of the intense heating pattern observed on the centerbody (see fig. 6) and should give a flow distribution representative of that existing where ignition occurs in the flow with injection. The general trend and magnitude of the measured and calculated test-gas flow distributions are quite similar. Apparently, the uniform test-gas flow produced by the nozzle contour which exists at the step is distorted by the swept expansion process that occurs between the step and the ignition location. About 30 percent of the fuel is introduced through the perpendicular injectors at the step with a uniform distribution like the test-gas flow there; the bulk of the fuel is introduced through the parallel injectors which are evenly spaced along the trailing edge of the centerbody where the test-gas flow has already been dis-

torted by the swept-expansion process. Once created by the swept expansion, this flow distortion persists even though intense mixing and reaction occur farther downstream between the trailing edge of the centerbody and the exit plane of the combustor duct.

Heating the fuel supplied to the perpendicular injectors from 300 K to 450 K to reduce differences in fuel temperature between the top and bottom of the flow reduces the flow distortion but does not eliminate it. Elimination of this flow distortion would require ignition and reaction of the fuel injected along the step such that a nearly constant static pressure would be maintained from the step to the trailing edge of the injector centerbody. In an actual engine the distributions of both perpendicular and parallel fuel injection along the strut may require tailoring to account for air flow distributions caused by the three-dimensional inlet process, as well as distortions caused by end effects due to pressure gradients that occur between the perpendicular and parallel fuel-injector locations.

In addition to strip integrations which give distributions of fuel and test gas in one direction across the exit plane of the combustor duct, overall integral values of fuel mass flow, test-gas mass flow, etc., were determined from the survey data. The results of these integrations are presented in table III, along with nominal bulk or measured test parameters for the Mach 1.7 nozzle contour and the Mach 1.3 nozzle contour. Note that the total flow in the combustor exit plane agrees with the measured flow input to the test-gas burner and fuel injectors within 5 percent for the Mach 1.7 and the Mach 1.3 data with ambient fuel temperature for which six surveys are available. Considering the number of measurements and assumptions involved, this level of agreement is acceptable. Also, the overall equivalence ratio determined from the integration is within 9 percent of the nominal value used for the data; again, this level of agreement is acceptable.

Comparison of survey results with one-dimensional analysis.- An estimate of the integral flow properties at the combustor duct exit can be made with a simplified one-dimensional analysis of the combustor flow. Starting with the flow conditions at the step, the one-dimensional conservation equations for mass, momentum, and energy are solved in a stepwise manner along the duct. The fraction of injected fuel reacted in each increment is adjusted to match the measured wall pressure distribution, and an estimate of the fuel reaction distribution and flow properties with distance along the combustor is obtained. Details of the analysis and assumptions are contained in references 9 and 10. The measured wall pressure distributions for the Mach 1.7 nozzle contour and the Mach 1.3 nozzle contour are shown in figures 14(a) and 14(b). Distance is measured from the step location, and in the fuel-injector section the spread of data represents the wall pressure variation observed in the sweep direction in the contour plots presented in figures 5(c) and 7(c). The data fairing in figures 14(a) and 14(b) is used for the one-dimensional analysis.

Values of the flow properties in the duct exit determined from the one-dimensional analysis are given in table III for comparison with the survey results, and the distribution of reaction with length obtained from the one-dimensional analysis is shown in figure 15. The results are plotted as overall combustion efficiency as a function of distance from the step nondimensionalized

by the total flow width ahead of the step (this width is equivalent to the gap between the center and side struts in the engine design). For both the Mach 1.7 nozzle contour and the Mach 1.3 nozzle contour the amount of fuel reacted rises steadily with distance, thus following similar trends. The combustion efficiency at the end of the duct determined from the one-dimensional analysis is 5 percent less than the integral value determined from the survey data in both cases. This close agreement implies that the local reaction parameter determined from the gas sample data is representative of the reaction existing in the flow, even though the sample acquisition process did not quench reaction. Thus, local chemical equilibrium is a good approximation for flow at the exit of the combustor duct at these test conditions, and the amount of reaction achieved is principally limited by the extent of mixing. Completion of reaction depends on completion of mixing before expanding the flow to lower static pressures and temperatures which would quench chemical reaction.

In the present tests, mixing efficiency of about 75 percent was achieved for both Mach numbers (see table III) in a length corresponding to 58 percent of the combustor length provided in the scramjet module design ($x/h = 48$). Extrapolating these data by using the computed results presented in reference 3 implies that combustion efficiencies of 90 to 95 percent should be obtained in the engine design. This estimate should be conservative since the end effect on the top wall (underside of the vehicle), which results in an overall nonuniform fuel-air distribution from top to bottom in this experiment, will affect a smaller portion of the flow as a result of the greater aspect ratio of the engine combustor entrance (22.5 for the engine versus 6.2 for the present experiment).

CONCLUDING REMARKS

The swept-injector model has proven to be a rapid and effective means for investigating some of the potential fuel injection and combustion problems which might be expected in tests of the complete Langley scramjet engine module at Mach 4 flight speeds. The test results show that once ignition is achieved at the perpendicular fuel-injection location, stable combustion can be maintained at stagnation temperatures corresponding to Mach 4 flight. With stoichiometric injection of ambient-temperature hydrogen fuel, an overall combustion efficiency of about 70 percent is achieved and no significant disturbances are generated ahead of the step. This implies high combustion efficiency should be obtained with the combustor length provided in the scramjet engine design and indicates no serious adverse combustor-inlet interactions should occur.

A significant end effect was observed between the step and the trailing edge on the top wall of the fuel-injector section (which corresponds to the underside of the vehicle in the engine module installation). In this region, the flow pattern without fuel injection causes a local increase in mass flux. Ignition of fuel introduced from the perpendicular injectors at the step occurs some distance downstream of the step along the top wall of the injector section near the trailing edge of the centerbody, but ignition occurs quite close to the step along the bottom wall. Because of this variation in ignition delay length from top to bottom, an increase in mass flux occurs near the top wall with fuel injection and combustion much like that without injection. This distortion of

the uniform flow existing upstream of the step occurs before the evenly spaced parallel injectors which are located on the trailing edge of the centerbody and supply most (70 percent) of the fuel added to the flow. The net result is that an overall nonuniform fuel and test-gas distribution was created which persisted to the exit of the combustor duct in spite of the intense mixing and chemical reaction that occurred between the trailing edge and the exit of the combustor duct. Increasing the temperature of the fuel supplied to the perpendicular injectors from 300 K to 450 K caused ignition to occur closer to the step near the top boundary; increasing the temperature reduced the extent of the end effect between the step and trailing edge and the size of the flow distortion at the combustor duct exit. However, for the model configuration with which heated-fuel tests were conducted (the Mach 1.3 nozzle contour), increased reaction near the step at the top wall led to significant pressure disturbance upstream of the step. Thus, it appears that achieving ignition close to the step (i.e., along a line of the same sweep as the step) and controlling the amount of reaction with distance (pressure gradient) will both be required to eliminate the flow distortion completely. The addition of ignition aids, tailoring the fuel injector pattern, and/or special aerodynamic contouring may all be necessary to eliminate this end effect without disturbing the flow upstream of the step.

From the point of view of the engine designer, tailoring the fuel-injection distribution to match the air flow distribution created from top to bottom along the struts by the inlet compression process will be required in any case. Also, elimination of the end effect may not be required since it covers less than one-third of the combustor duct exit plane which corresponds to less than 10 percent of the engine flow cross section. The principal result of the tests presented here is that stable combustion with reasonable efficiency and without adverse combustor-inlet interaction appears feasible for the engine design.

Langley Research Center
National Aeronautics and Space Administration
Hampton, VA 23665
May 25, 1977

APPENDIX

PROBE SURVEY DATA ACQUISITION AND ANALYSIS TECHNIQUE

As described in the main body of this report, combustor-duct-exit surveys are acquired with a nine-tube, water-cooled, pitot pressure and gas sample rake. (See ref. 11.) In a typical run the probe is inserted to a preselected position in the flow after steady test conditions have been established. With the rake stationary, pitot pressure is recorded for 1 to 2 sec; then a gas sample is acquired in the remaining 8 to 12 sec of the run. For the first 2 to 3 sec of this sample interval, gas from the probe tip flows through the (initially evacuated) sample bottle to a vacuum reservoir. This action is required to purge the line from the probe to the sample bottle. Then the exit valve on the sample bottle is closed, and the pressure is allowed to build up toward the pitot pressure level existing in the stream ahead of the probe tip. The bottle inlet valve is closed just before the run terminates. The sample bottle pressure generally reaches about two-thirds of pitot pressure and is usually greater than 1 atm (1 atm = 101 325 Pa).

With this sample acquisition procedure, it is likely that chemical reaction is completed as the sample enters the probe tip. After a test, each sample bottle is isolated by manual valves and is removed from the probe system; the contents are analyzed by a gas chromatograph at a location remote from the test apparatus. Details of the gas-chromatograph analysis technique are given in reference 11.

Since the probe, line, and sample bottle are all at approximately room temperature, most of the water content of the sample condenses. The chromatograph analysis determines the relative amounts of hydrogen, oxygen, and nitrogen in the remaining gaseous portion of the sample bottle contents. A mass balance calculation is then made with each dry sample composition to determine the wet composition that existed in the stream at the probe tip. In this calculation the measured flows of hydrogen, oxygen, and air supplied to the test gas burner are assumed to mix and react completely. Thus, the nitrogen supplied in the air can be used as an inert tracer for the test gas, and all wet sample compositions are calculated by using the test gas oxygen-to-nitrogen atom ratio computed from the measured oxygen and air flows supplied to the burner. The amount of water vapor in the test gas from combustion in the burner is determined by the measured flows to the burner. Additional water (and unburned hydrogen) is due to fuel injected in the swept-strut injector model. It is assumed that all transport processes are turbulent so that each sample is a mixture of test gas (whose composition is known from the measured flows supplied to the burner) and hydrogen fuel injected in the test model.

Data from a single test firing are put in nondimensional form with fuel mass fraction divided by the average fuel mass fraction (calculated from the measured hydrogen and test-gas flow rates) and pitot pressure divided by the test-gas burner stagnation pressure. The amount of reaction in each sample is specified in dimensionless form by the fraction of the least available reactant consumed. This choice of dimensionless variables is advantageous because the exit-plane properties are assembled with data from several test firings. Small

differences in fuel flow rate, test-gas oxygen content, and burner pressure occur from run to run; and by choosing this particular dimensionless representation of the data, the effect of these differences on property contour maps and integrated parameters is minimized.

Survey data at locations covering the exit plane from several test firings are input to a computer program, created by Charles J. Schexnayder and John S. Evans, named COPEIN (COmbustion PErformance INtegration) along with the nominal test conditions, survey locations, exit plane geometry, etc. The first portion of COPEIN uses a surface spline routine (described in ref. 12) to make a smooth fit of the probe data (the dimensionless values of fuel concentration, reaction efficiency, and pitot pressure) over the entire exit plane. The surface spline routine makes use of the small deflection equation of an elastic plate pinned at the data points in generating the data fit. The boundaries of the exit plane are treated like planes of symmetry by adding as data points the values measured closest to the boundary at an equal distance outside the boundary.

Once the data fit has been generated, three 20 × 20 arrays of values corresponding to a uniformly spaced grid over the entire exit plane are established to represent the measured data. At each of these 400 grid points all other flow properties desired are then calculated. The flow is assumed to have uniform static pressure equal to the value measured at the end of the combustor duct. Heat loss to the test-gas burner and combustor model are subtracted uniformly from the entire flow. With this assumption and the assumption of entirely turbulent transport (including heat transport) in the flow, the total enthalpy can be calculated at each point from the test-gas composition, fuel concentration, and reaction efficiency. Gas properties are computed by assuming no dissociation (i.e., only water is formed as a combustion product) with real-gas specific heats for each specie present. An iterative calculation is used to determine velocity from the local pitot pressure and the uniform exit-plane static pressure. As properties at each grid point are calculated, appropriate sums for the strip integrations and overall integrations are accumulated. Arrays of values for which contour plots are desired are also formed. The contour plots are constructed by the same code which was used to make the wall static-pressure contour plots presented in figures 5 and 7. (See ref. 7.)

A large number of trial calculations were performed with one set of probe data to test the sensitivity of the integrated and property contour results to possible errors in the various input parameters required for the calculation. Perhaps surprisingly, it was found that the integrated parameters such as test-gas and injected-fuel flows are relatively insensitive to variations in duct exit static pressure, heat loss, test-gas composition, etc. Fairly large changes in these input parameters produced only small changes in the integrated results. More important, ratios of integrated parameters such as the overall equivalence ratio and overall combustion efficiency appear to be essentially independent of parameters such as duct-exit static pressure, etc. These ratios appear to be determined almost solely by the probe survey data. Of course, as would be expected for an integration procedure, large changes in the probe survey data in a small part of the exit plane produce only small changes in the overall integrated result. All in all, the COPEIN integration program appears to be an accurate and powerful tool for displaying and evaluating the detailed flow survey data obtained from combustion experiments.

REFERENCES

1. Henry, John R.; and Anderson, Griffin Y.: Design Considerations for the Airframe-Integrated Scramjet. NASA TM X-2895, 1973.

2. Trexler, Carl A.: Inlet Performance of the Integrated Langley Scramjet Module (Mach 2.3 to 7.6). AIAA Paper No. 75-1212, Sept.-Oct. 1975.

3. Anderson, Griffin Y.: An Examination of Injector/Combustor Design Effects on Scramjet Performance. NASA paper presented at the 2nd International Symposium on Air Breathing Engines (Sheffield, England), Mar. 25-29, 1974.

4. Kalben, P.: A FORTRAN Program for the Determination of Nozzle Contours for Rotational, Non-Homentropic Gas Mixtures. ATL TM 148 (Contract NAS1-9560), Advanced Technology Lab., Inc., Mar. 1970. (Available as NASA CR-145196.)

5. Russin, William Roger: Performance of a Hydrogen Burner To Simulate Air Entering Scramjet Combustors. NASA TN D-7567, 1974.

6. Rogers, R. C.; and Eggers, J. M.: Supersonic Combustion of Hydrogen Injected Perpendicular to a Ducted Vitiated Airstream. AIAA Paper No. 73-1322, Nov. 1973.

7. Wright, Thomas J.: Utility Plotting Programs at NCAR. Atmos. Technol., no. 3, Sept. 1973, pp. 51-57.

8. Salas, Manuel D.: Shock Fitting Method for Complicated Two-Dimensional Supersonic Flows. AIAA J., vol. 14, no. 5, May 1976, pp. 583-588.

9. Anderson, Griffin Y.; and Gooderum, Paul B.: Exploratory Tests of Two Strut Fuel Injectors for Supersonic Combustion. NASA TN D-7581, 1974.

10. Anderson, Griffin Y.; Eggers, James M.; Waltrup, Paul J.; and Orth, Richard C.: Investigation of Step Fuel Injectors for an Integrated Modular Scramjet Engine. 13th JANNAF Combustion Meeting, Volume III, CPIA Publ. 281 (Contract N00017-72-C-4401), Appl. Phys. Lab., Johns Hopkins Univ., Dec. 1976, pp. 175-189.

11. Eggers, James M.: Composition Surveys of Test Gas Produced by a Hydrogen-Oxygen-Air Burner. NASA TM X-71964, 1974.

12. Harder, Robert L.; and Desmarais, Robert N.: Interpolation Using Surface Splines. J. Aircr., vol. 9, no. 2, Feb. 1972, pp. 189-191.

TABLE I.- MINIMUM TEST-GAS STAGNATION TEMPERATURES FOR AUTOIGNITION OF FUEL FROM PERPENDICULAR INJECTORS

Nozzle contour	Burner stagnation conditions		Static-flow conditions at step		Test-gas stagnation temperature, K
	Pressure, MPa	Temperature, K	Pressure, MPa	Temperature, K	
Mach 1.7	0.8 to 0.5	1180	0.18 to 0.12	805	300
Mach 1.3	.8	1150	.34	924	300
Mach 1.3	.8	1010	.34	811	435

TABLE II.- BURNER OPERATING CONDITIONS

f	I	$p_{t,h}$, MPa	$T_{t,h}$, K	w_h, kg/sec	w_j, kg/sec	$\bar{\phi}$ (*)	z	Figure
Mach 1.7 nozzle contour								
0.0073	1.02	0.836	964	3.52	0.109	1.01	0.50	9
.0073	1.03	.842	962	3.48	.111	1.03	.25	9
.0072	1.03	.852	958	3.53	.110	1.00	.88	5(c) and 9
.0074	1.01	.858	975	3.55	.113	1.00	.63	9
.0075	1.01	.852	995	3.54	0	0		5(a)
.0075	1.01	.856	987	3.52	.045	.43		5(b)
.0075	1.00	.845	993	3.46	.108	1.01	.10	9 and 14(a)
.0075	1.01	.853	986	3.47	.105	.98	.31	9
Mach 1.3 nozzle contour								
0.0073	1.02	0.789	991	4.14	0.128	1.00	0.29	10
.0072	1.04	.785	1001	4.10	.127	1.00	.65	10
.0073	1.00	.781	1006	4.07	.126	1.00	.79	10 and 14(b)
.0074	1.02	.783	1016	4.05	.123	.99	.43	10
.0072	1.01	.788	996	4.10	.125	.99	.14	7(c) and 10
.0072	1.04	.780	1005	4.05	.125	1.00	.93	10
.0076	1.04	.752	1035	3.96	0	0		7(a)
.0075	1.00	.781	1029	4.01	.042	†.35		7(b)
.0073	1.01	.793	1004	4.06	.133	†1.09	.50	7(d) and 11
.0074	.97	.793	1020	4.05	.126	†1.03	.39	11
.0074	.99	.786	1020	4.06	.127	†1.04	.28	11

*$\bar{\phi} = w_j/w_h/0.03$; fuel split, 30-percent perpendicular injection and 70-percent parallel injection.

†Heated fuel runs, $T_{t,j} \approx 450$ K for perpendicular injection; all other runs, $T_{t,j} \approx 300$ K.

TABLE III.- COMPARISON OF COMBUSTOR EXIT-FLOW PROPERTIES

Parameter	Mach 1.7 nozzle contour			Mach 1.3 nozzle contour			
	Bulk or measured	Survey integration	One-dimensional calculation	Bulk or measured	Survey integration	Heated-fuel survey integration	One-dimensional calculation
f	0.007	[a]0.007	[a]0.007	0.007	[a]0.007	[a]0.007	[a]0.007
I	1.0	[a]1.0	[a]1.0	1.0	[a]1.0	[a]1.0	[a]1.0
$p_{t,h}$, MPa	0.827		[a]0.827	0.793			[a]0.793
$T_{t,h}$, K	941		[a]941	973			[a]973
w_h, kg/sec	3.47	3.29	[a]3.47	4.18	3.98	3.83	[a]4.18
w_j, kg/sec	0.102	0.0903		0.123	0.117	0.120	
$\bar{\phi}$	1.0	0.91	[a]0.91	1.0	0.97	1.01	[a]0.97
Q, MJ/sec	[b]0.25	[a]0.25	0.25	[b]0.3	[a]0.3	[a]0.3	0.3
η_c		0.76	0.71		0.72	0.78	0.67
η_m		0.77	1.0		0.77	0.82	1.0
E_r		0.98	1.0		0.93	0.95	1.0
F/w, m/sec		1774	1825		1856	1976	1838
H, MJ/kg		5.201	5.180		5.438	5.807	5.453
M			1.56				1.70
K			0.91				0.81
C_f			[a]0.002				[a]0.002

[a]Input in data reduction.
[b]Estimated.

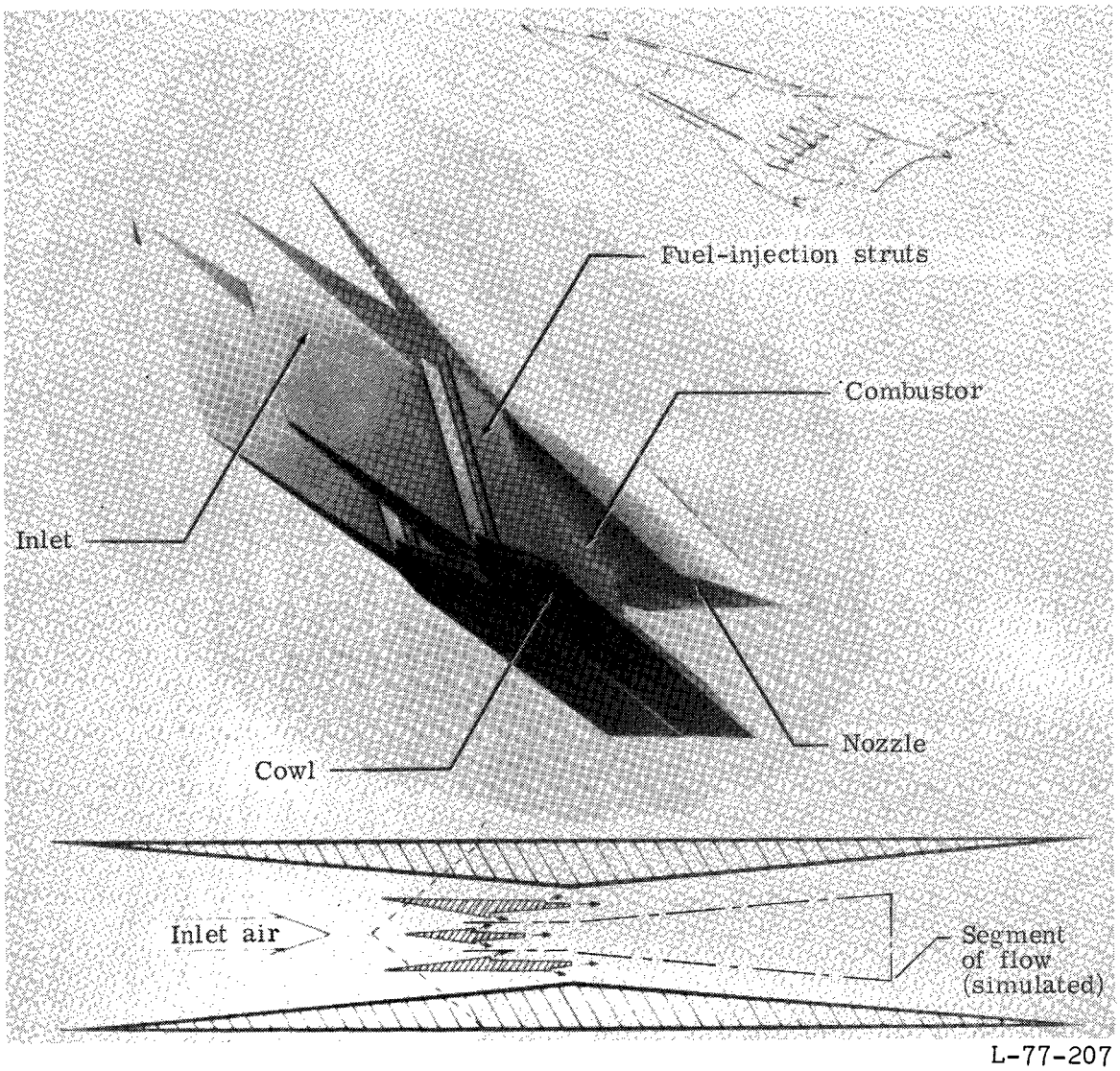

Figure 1.- Langley integrated modular scramjet engine.

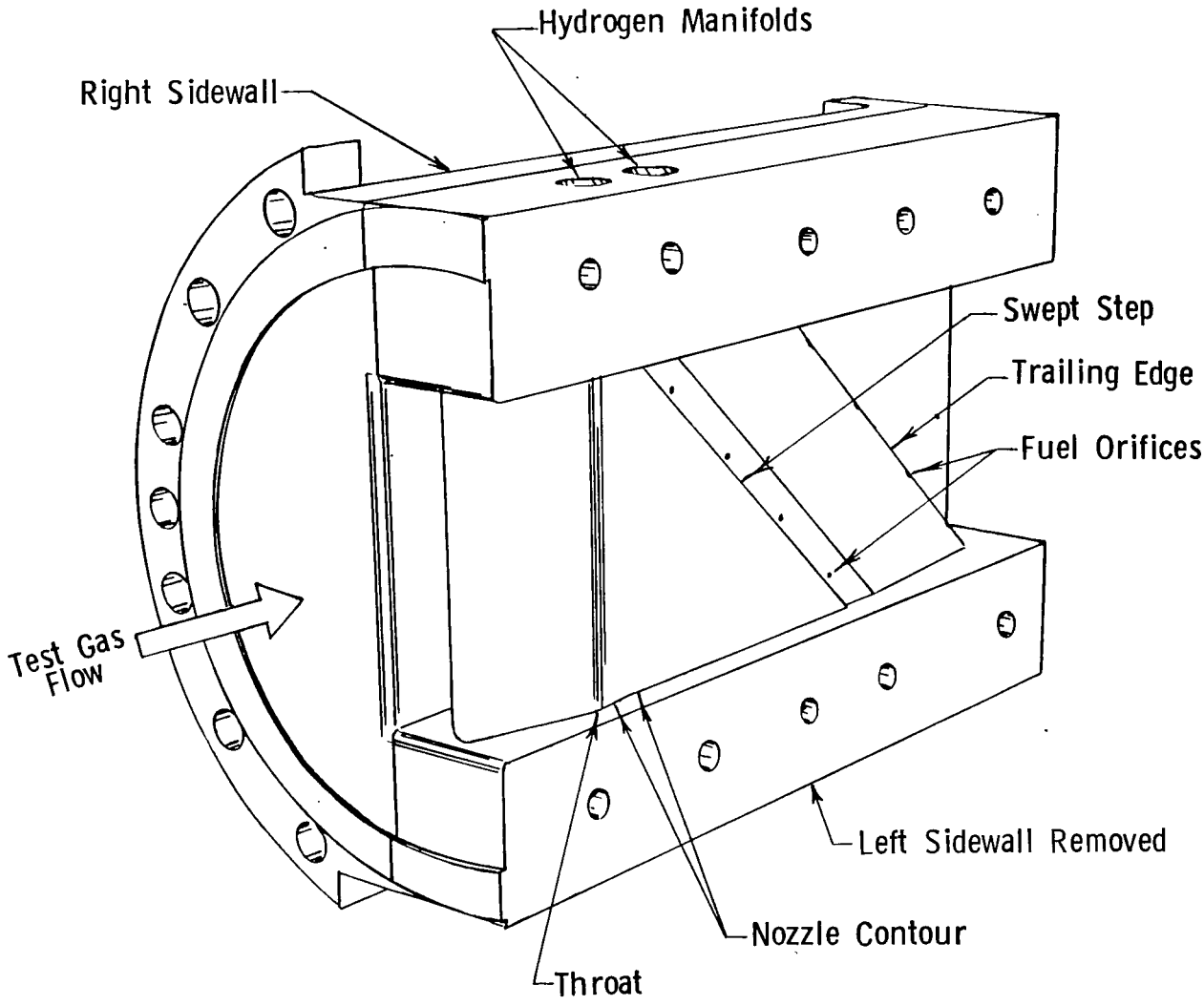

Figure 2.- Perspective view of swept-strut fuel injector.

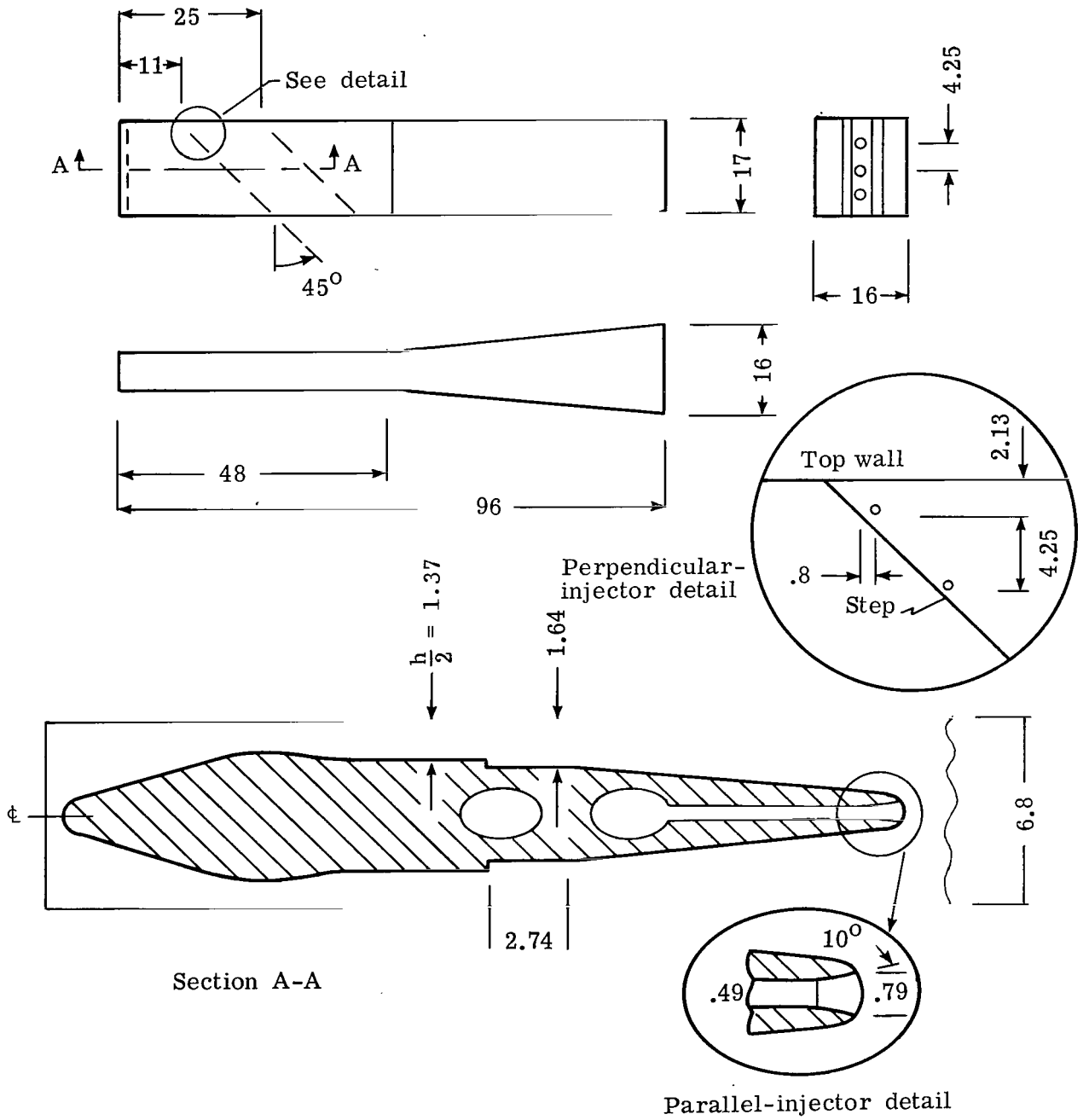

Figure 3.- Dimensions of swept-strut fuel injector. All dimensions are in cm.

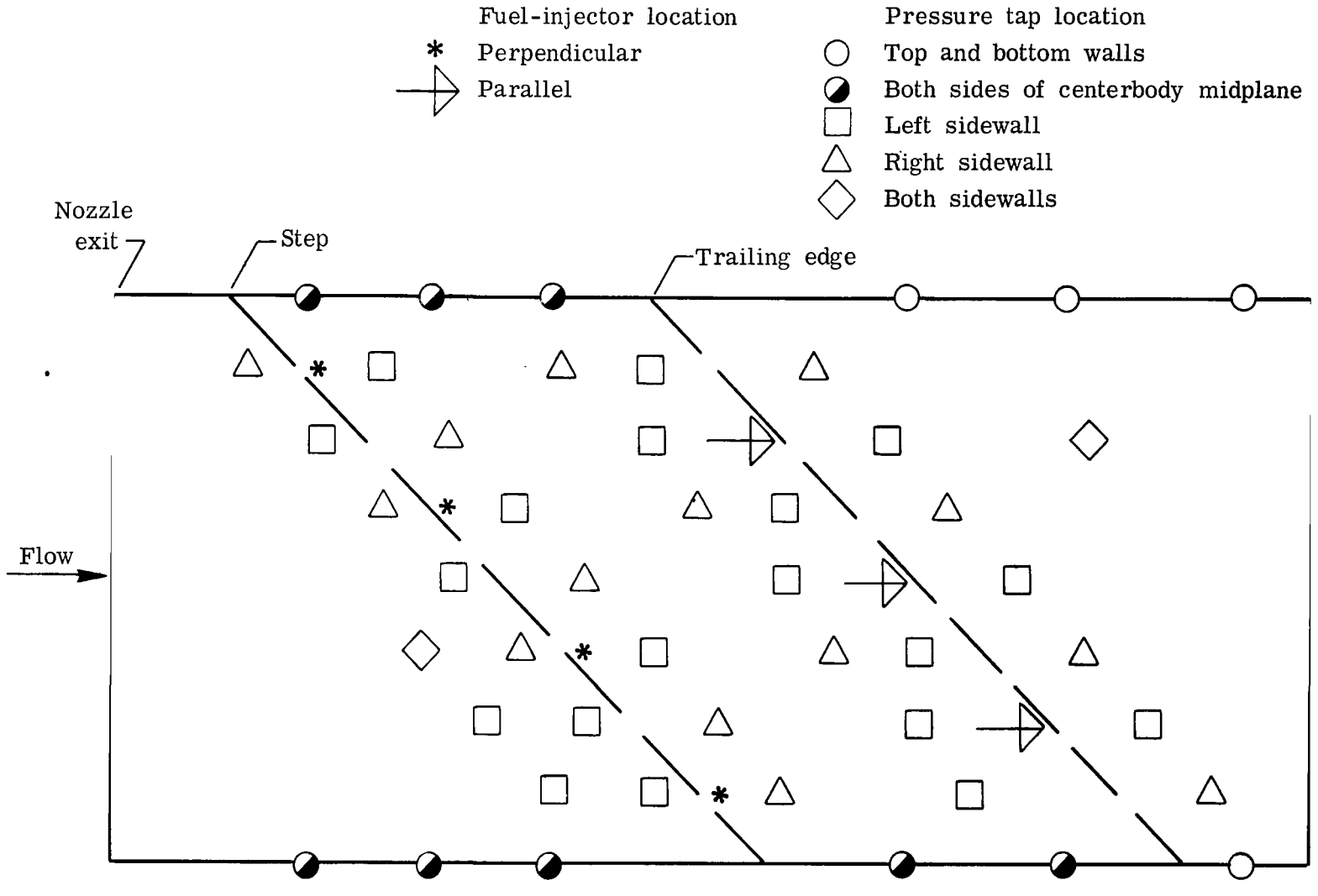

Figure 4.- Pressure tap locations of swept-strut fuel injector.

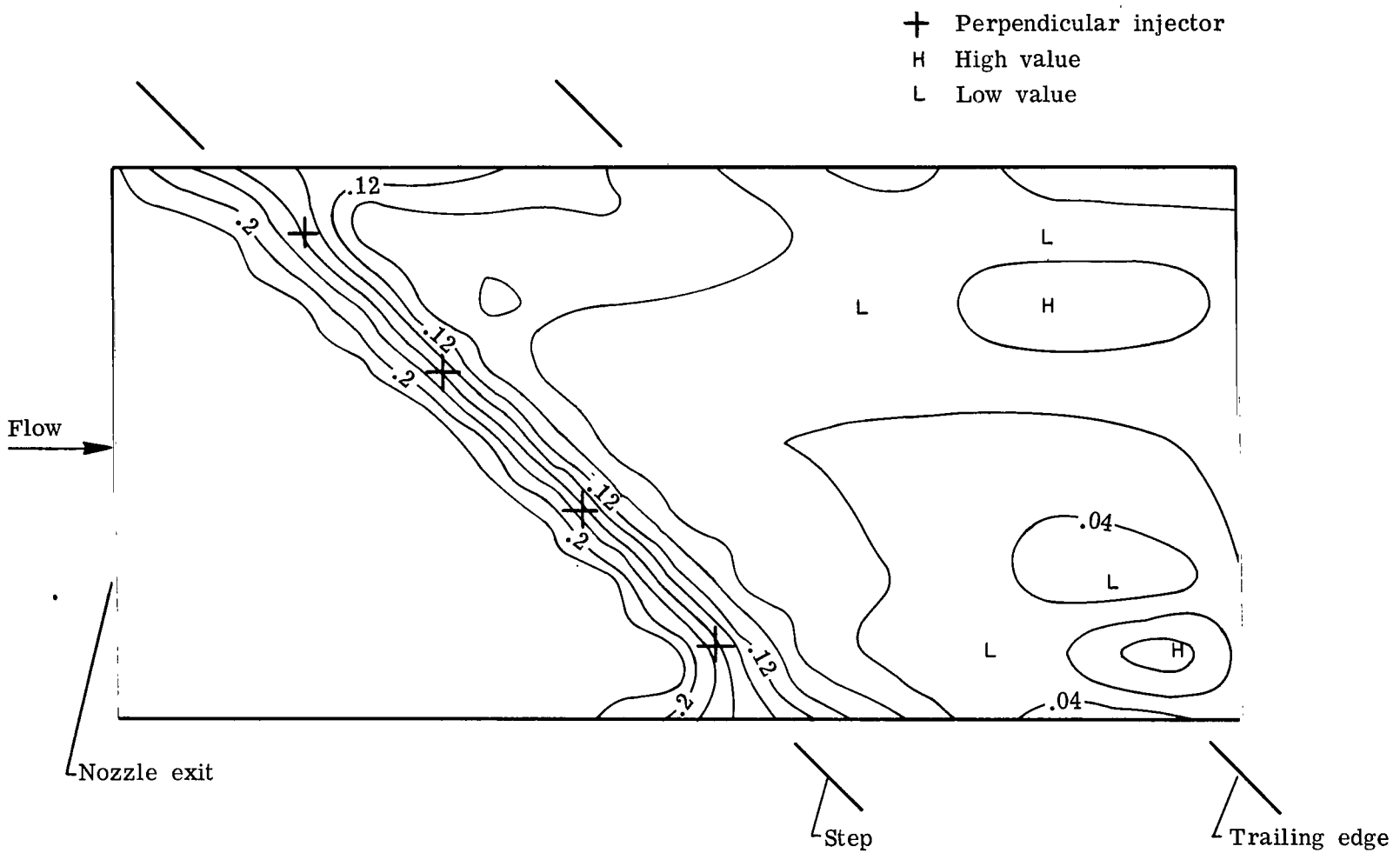

(a) $\bar{\phi}$ = 0; contours at 0.02 intervals.

Figure 5.- Dimensionless wall pressure pattern $p/p_{t,h}$ for Mach 1.7 nozzle contour.

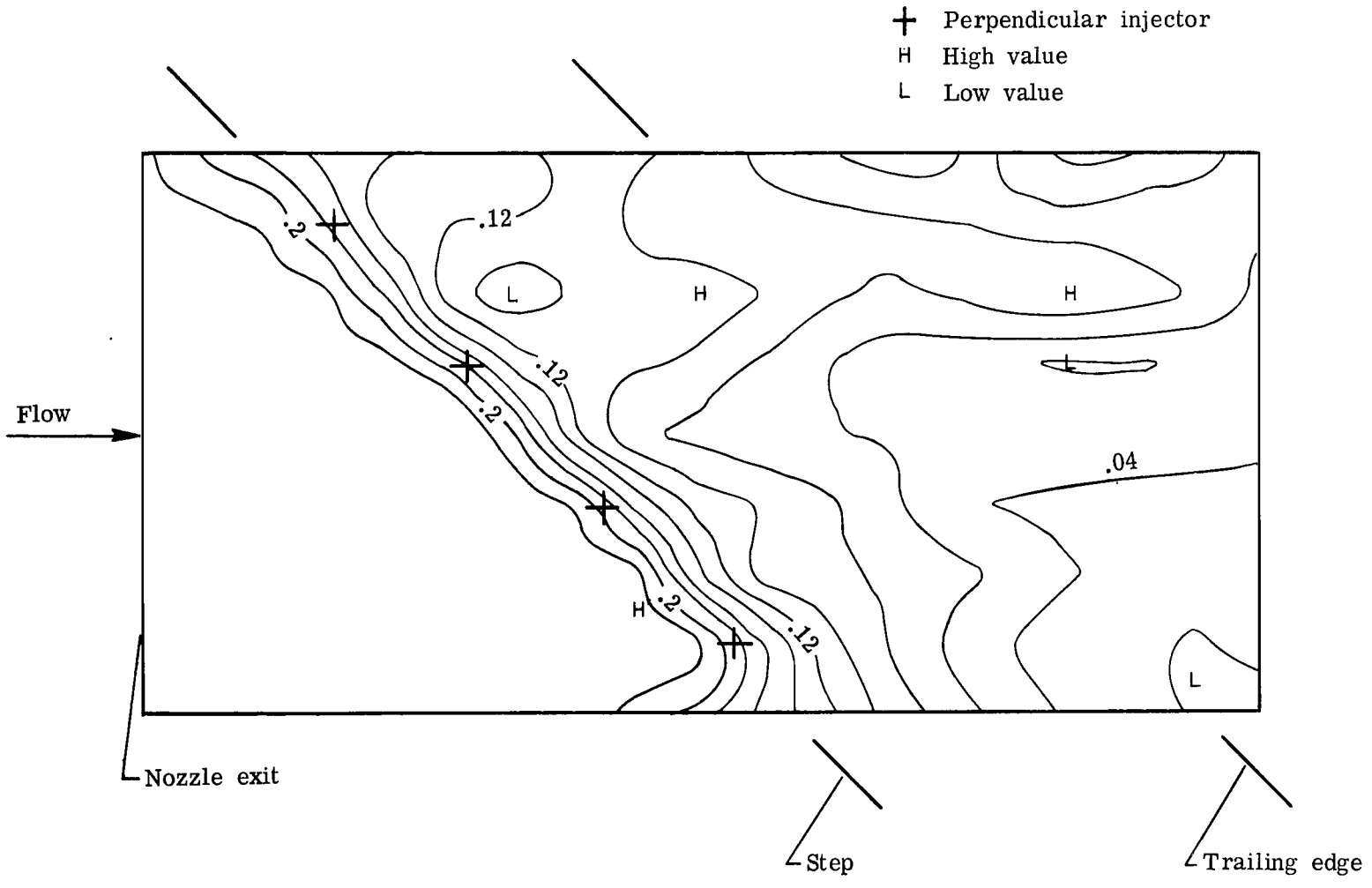

(b) Perpendicular injection; $\bar{\phi}$ = 0.43; contours at 0.02 intervals.

Figure 5.- Continued.

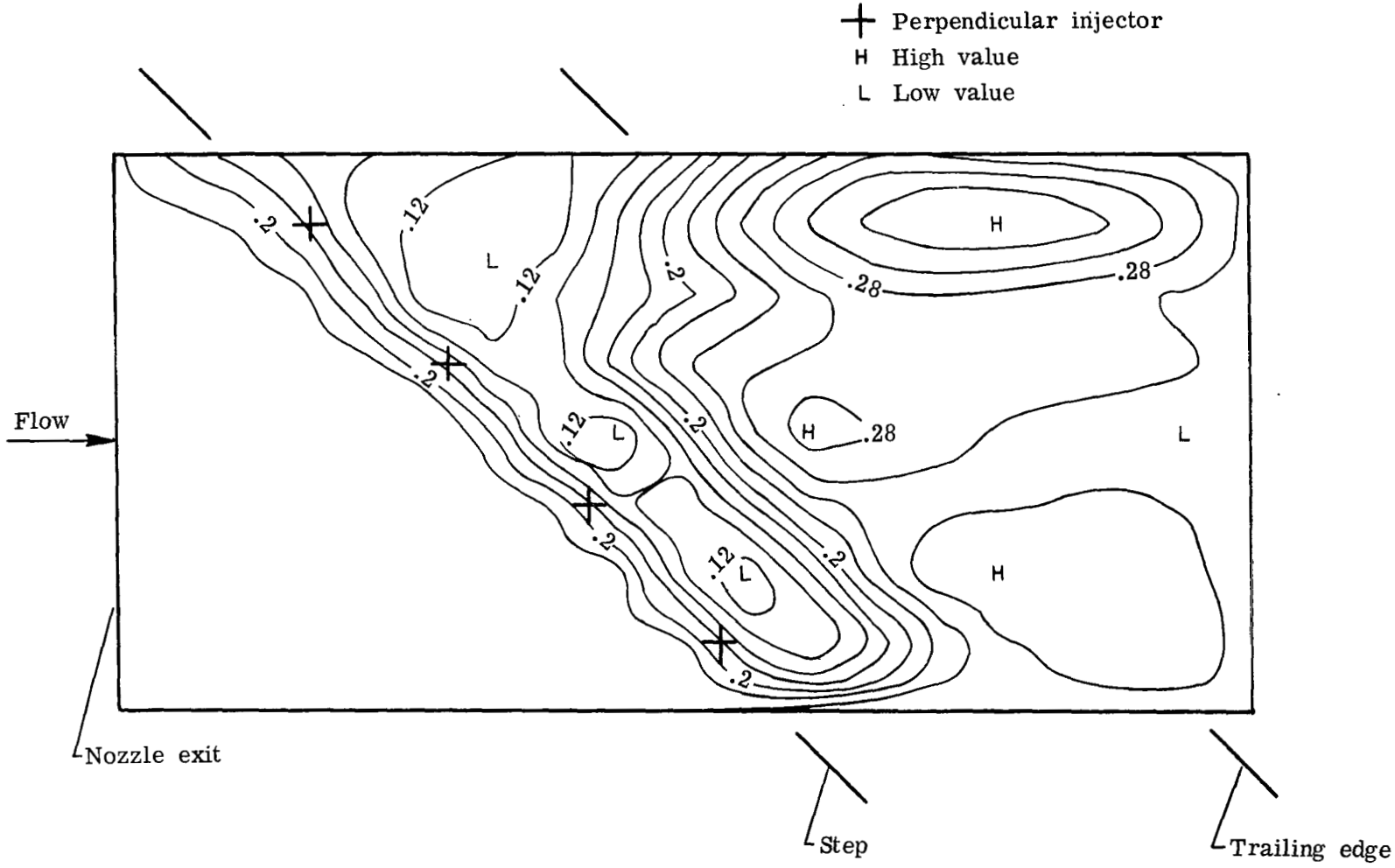

(c) Fuel split, 30-percent perpendicular and 70-percent parallel; $\bar{\phi} = 1$; contours at 0.02 intervals.

Figure 5.- Concluded.

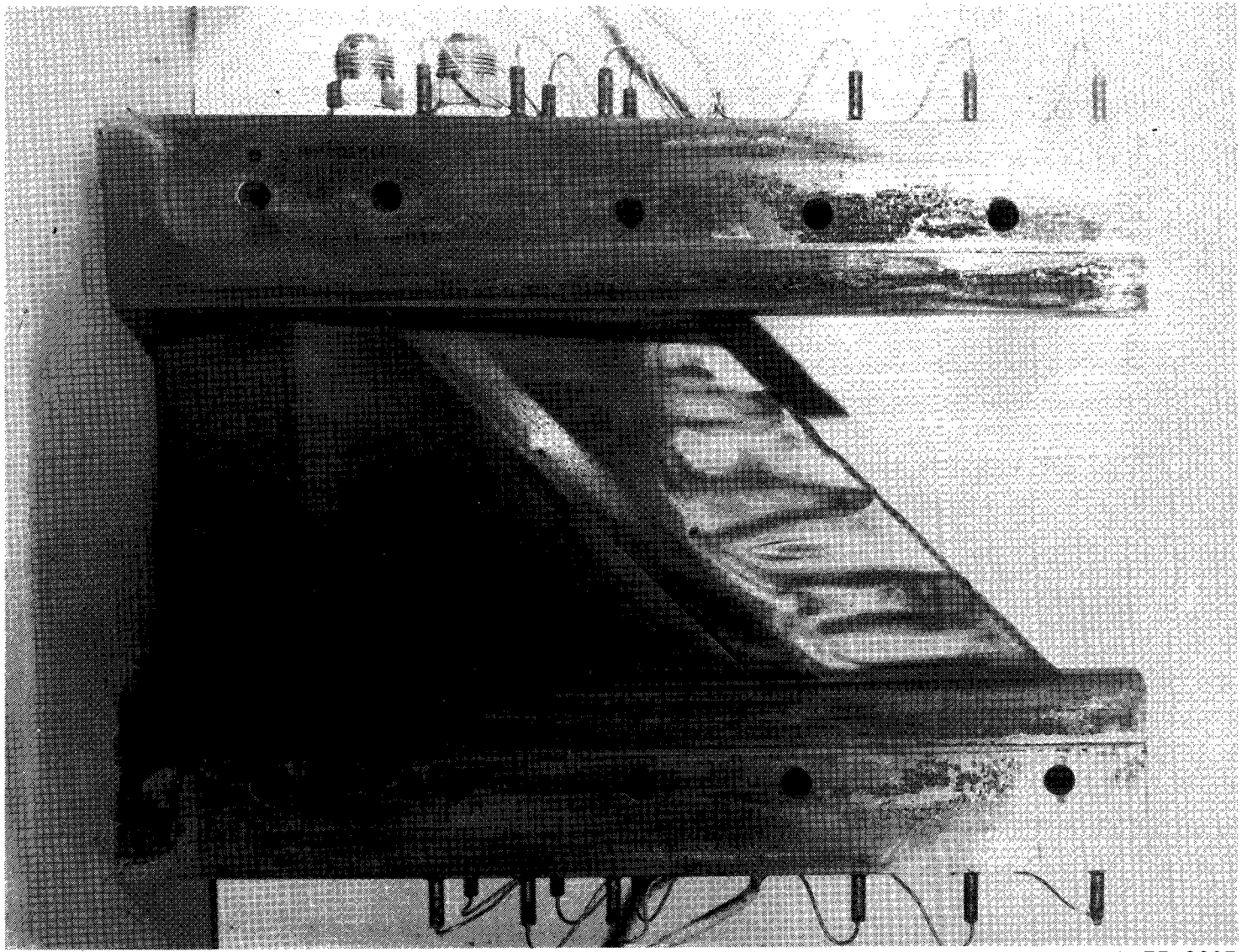

L-75-3327

Figure 6.- Heating pattern on injector centerbody after Mach 1.7 tests.

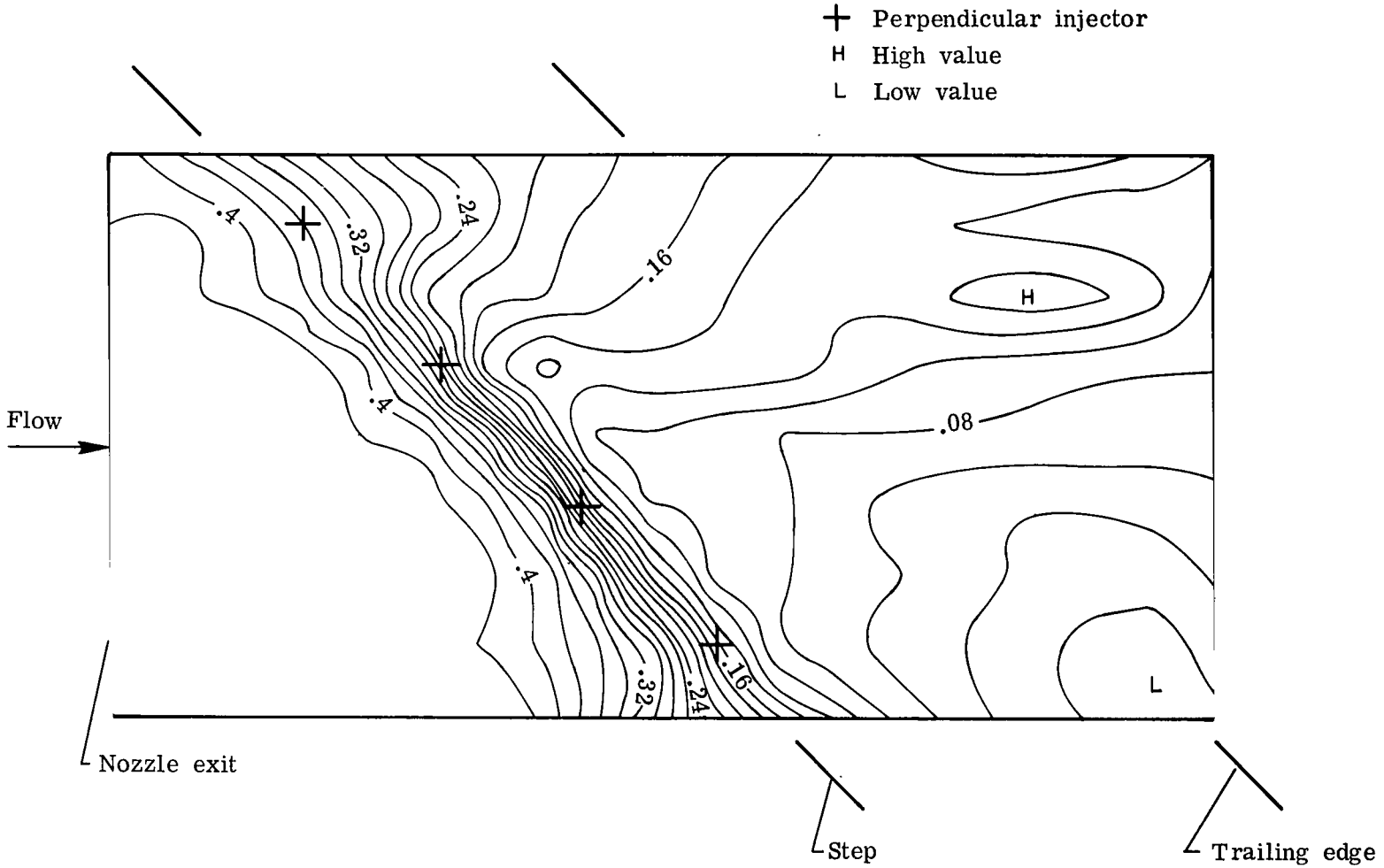

(a) $\bar{\phi} = 0$; contours at 0.02 intervals.

Figure 7.- Dimensionless wall pressure pattern $p/p_{t,h}$ for Mach 1.3 nozzle contour.

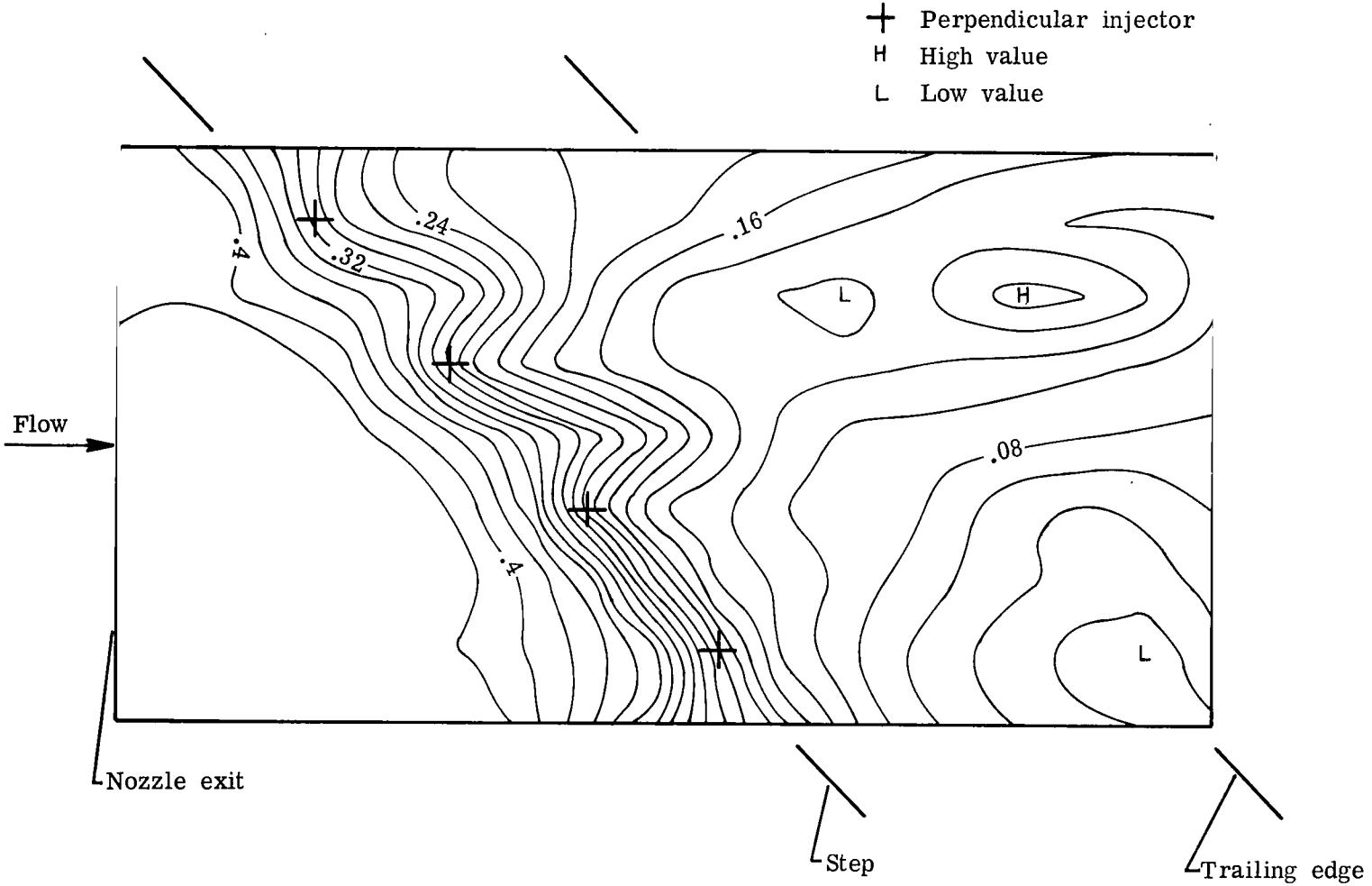

(b) Perpendicular injection; $\bar{\phi}$ = 0.35; contours at 0.02 intervals.

Figure 7.- Continued.

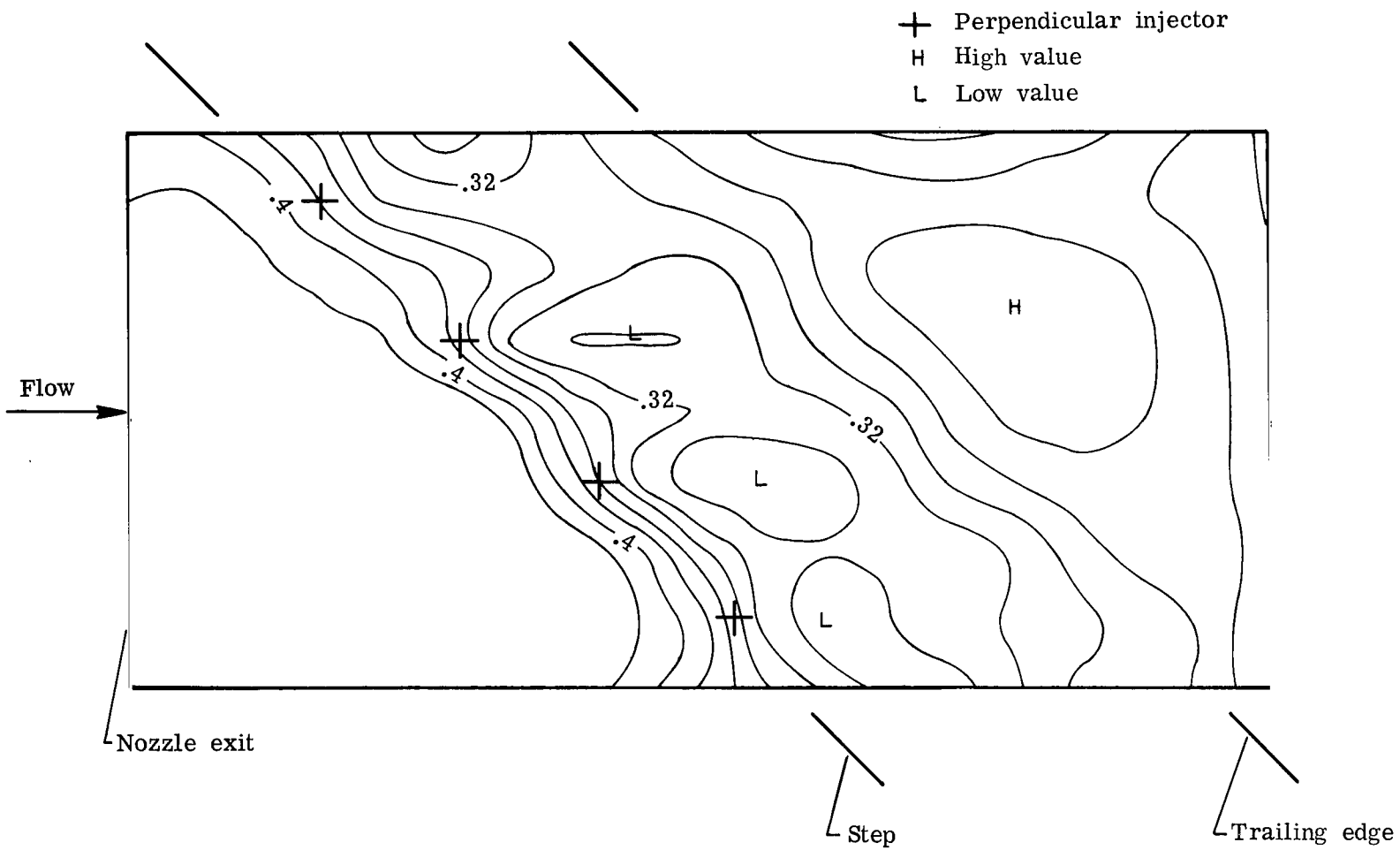

(c) Fuel split, 30-percent perpendicular and 70-percent parallel; $\overline{\phi}$ = 0.99; contours at 0.02 intervals.

Figure 7.- Continued.

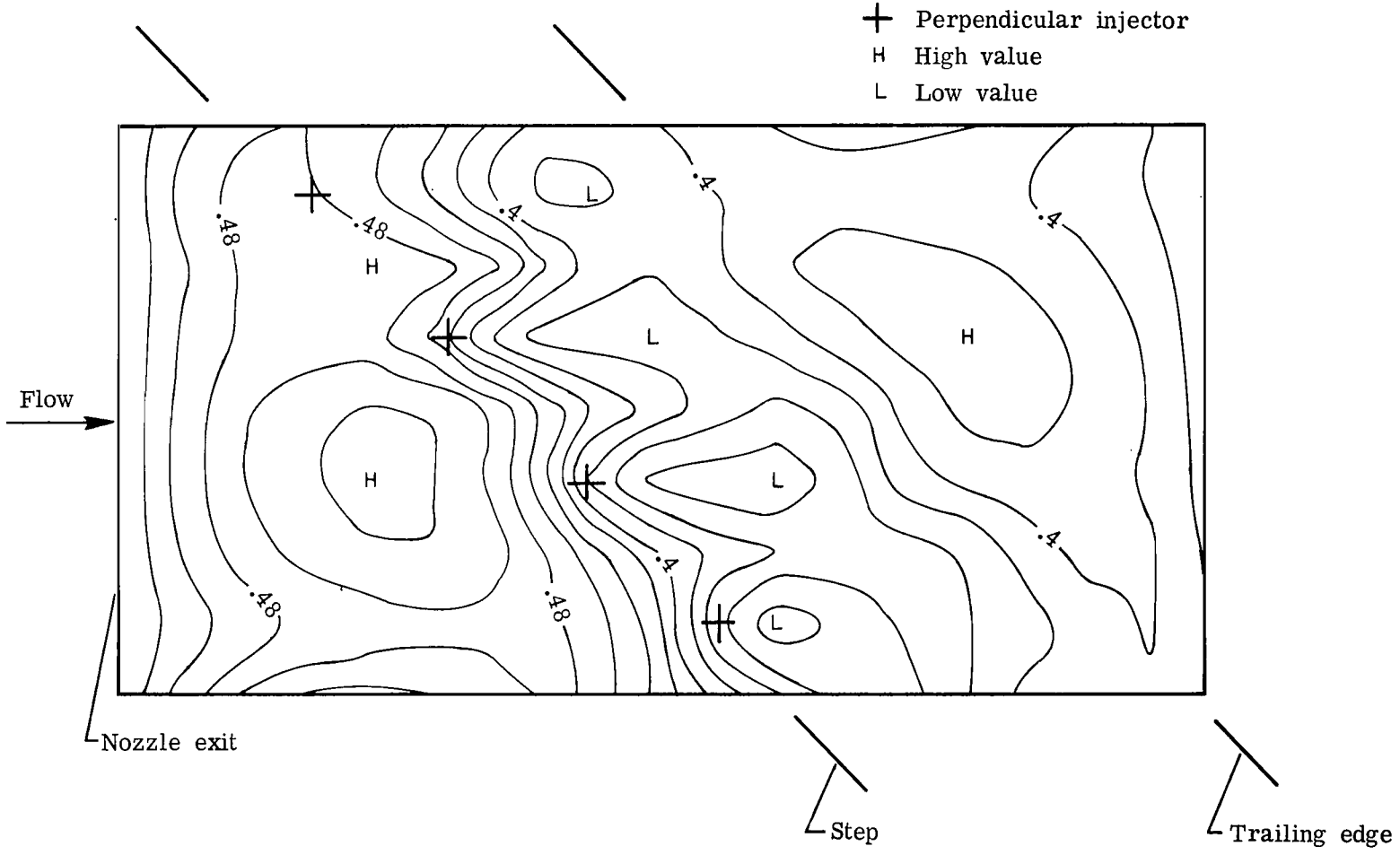

(d) Fuel split, 30-percent perpendicular and 70-percent parallel; $\bar{\phi}$ = 1.09; 450 K fuel supplied to perpendicular injectors; contours at 0.02 intervals.

Figure 7.- Concluded.

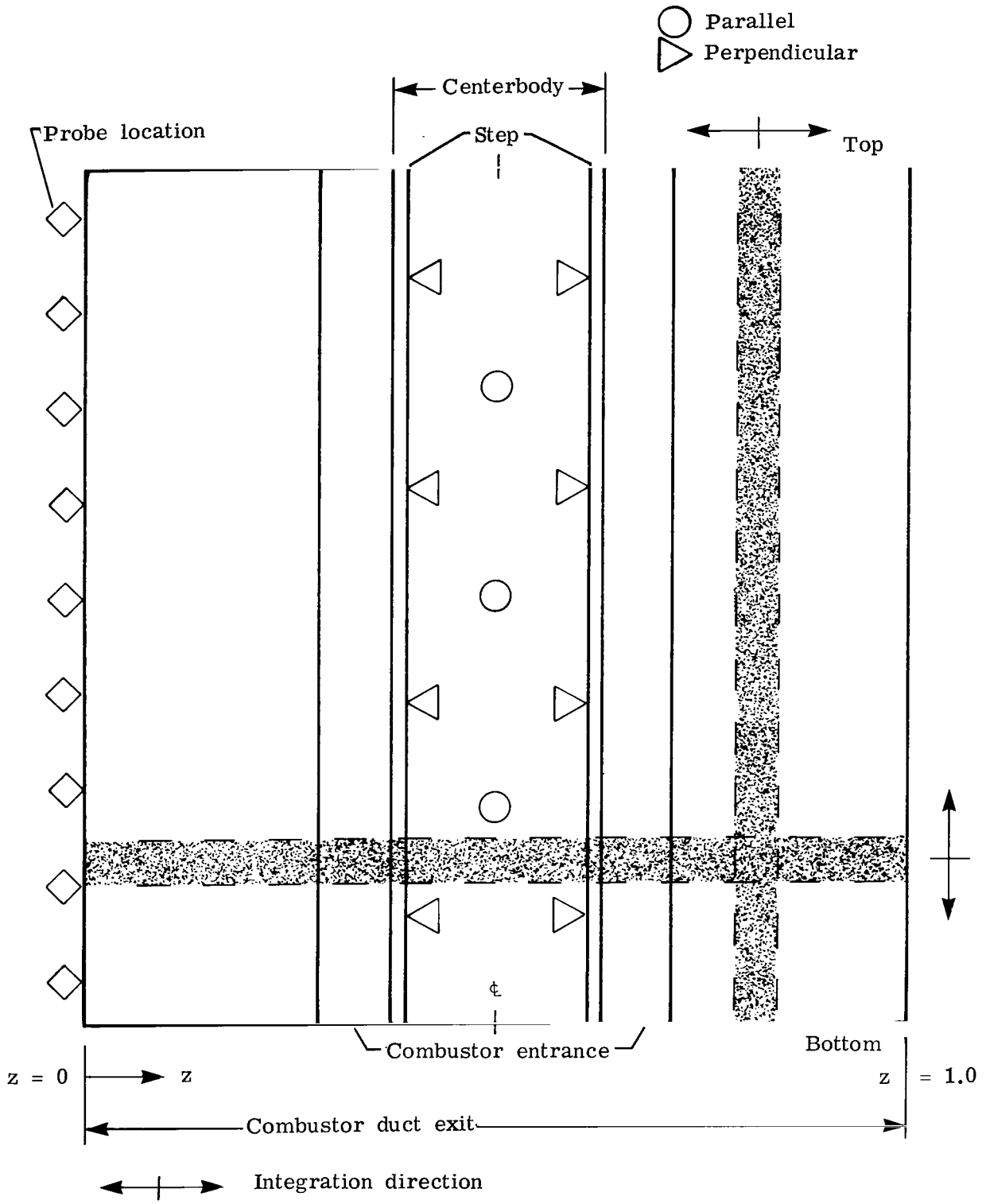

Figure 8.- Geometry of combustor duct exit plane.

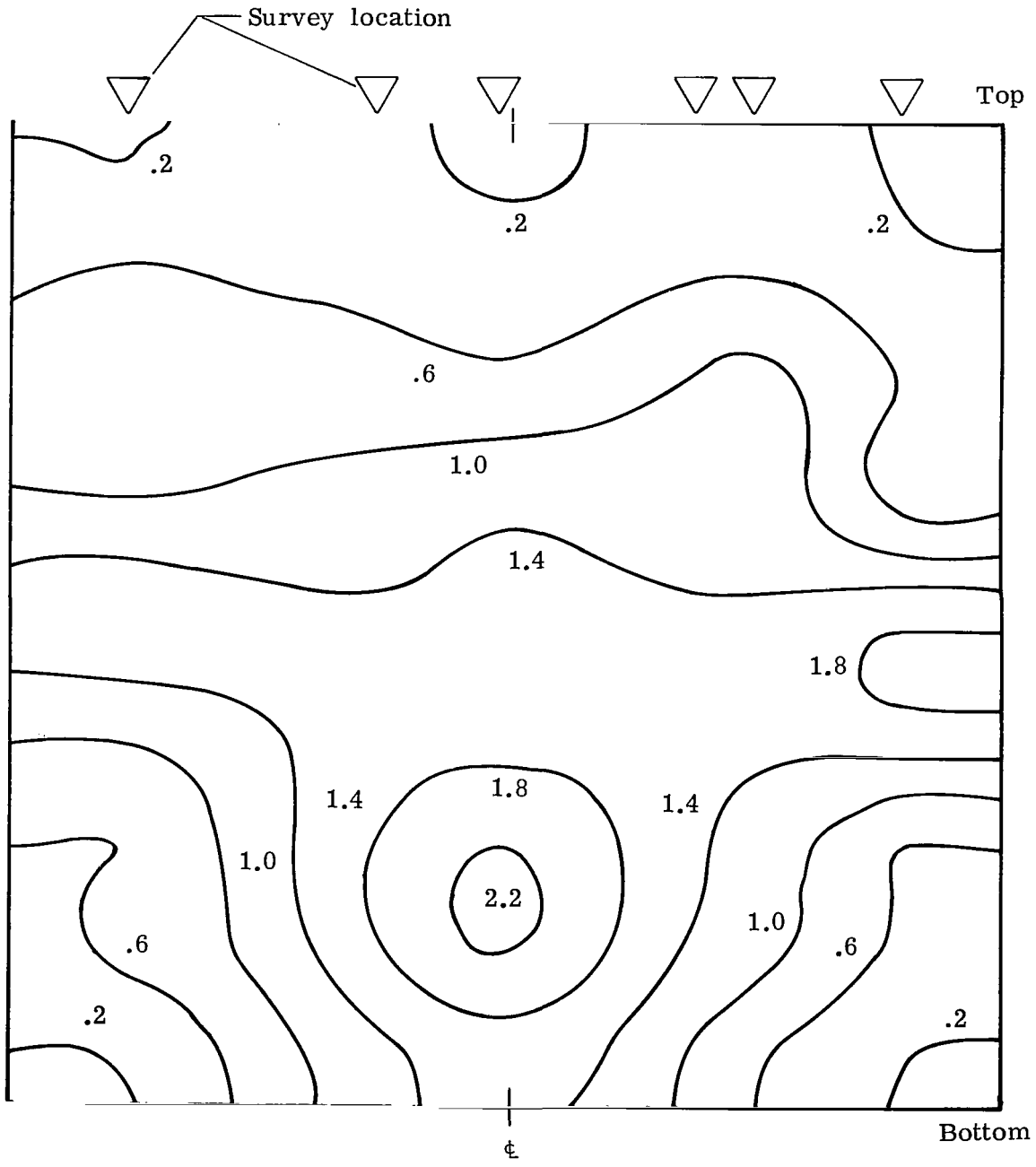

(a) Fuel distribution.

Figure 9.- Surveys of the exit plane of the combustor duct for Mach 1.7 nozzle contour; $\bar{\phi} = 1$.

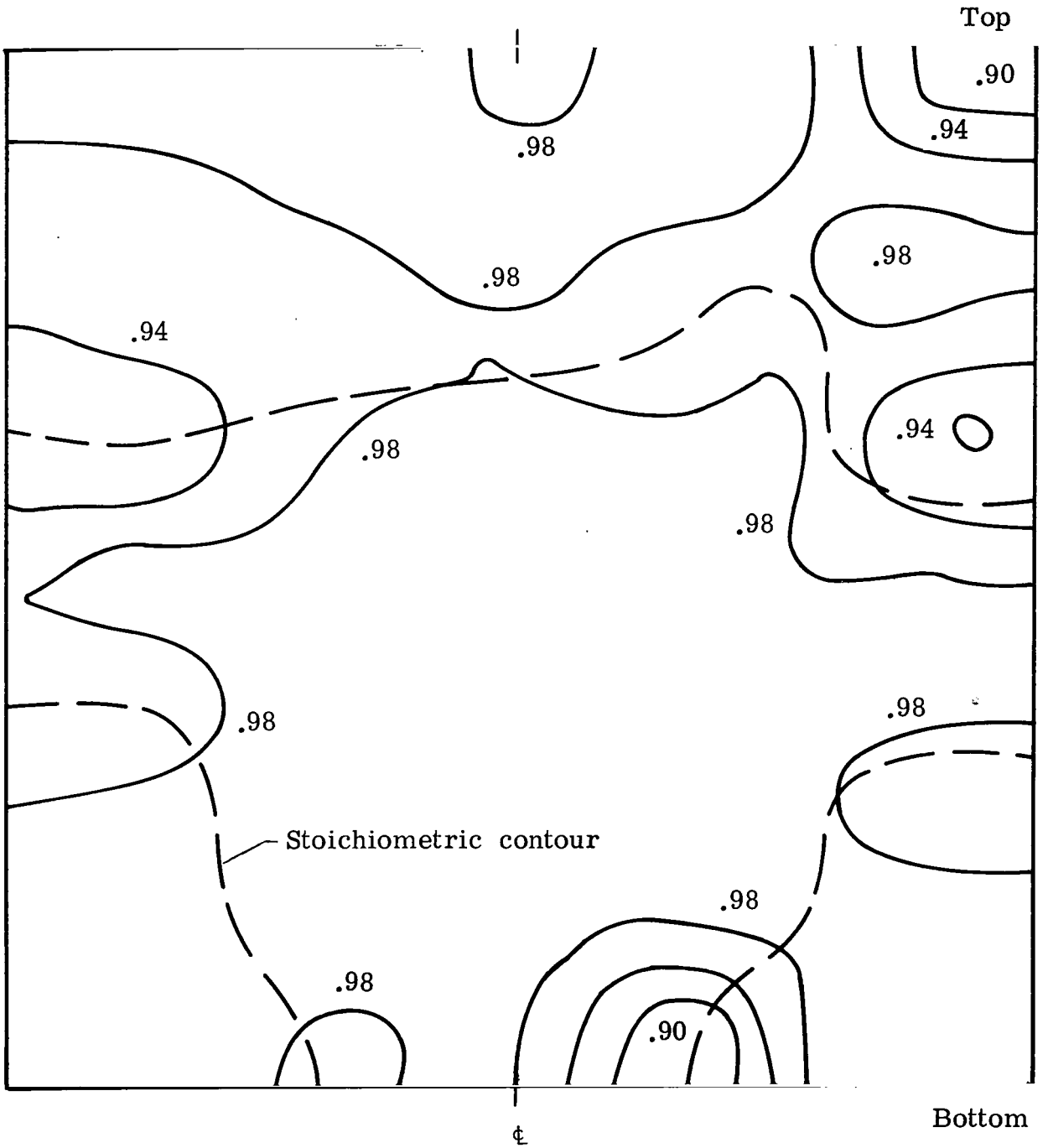

(b) Reaction distribution.

Figure 9.- Continued.

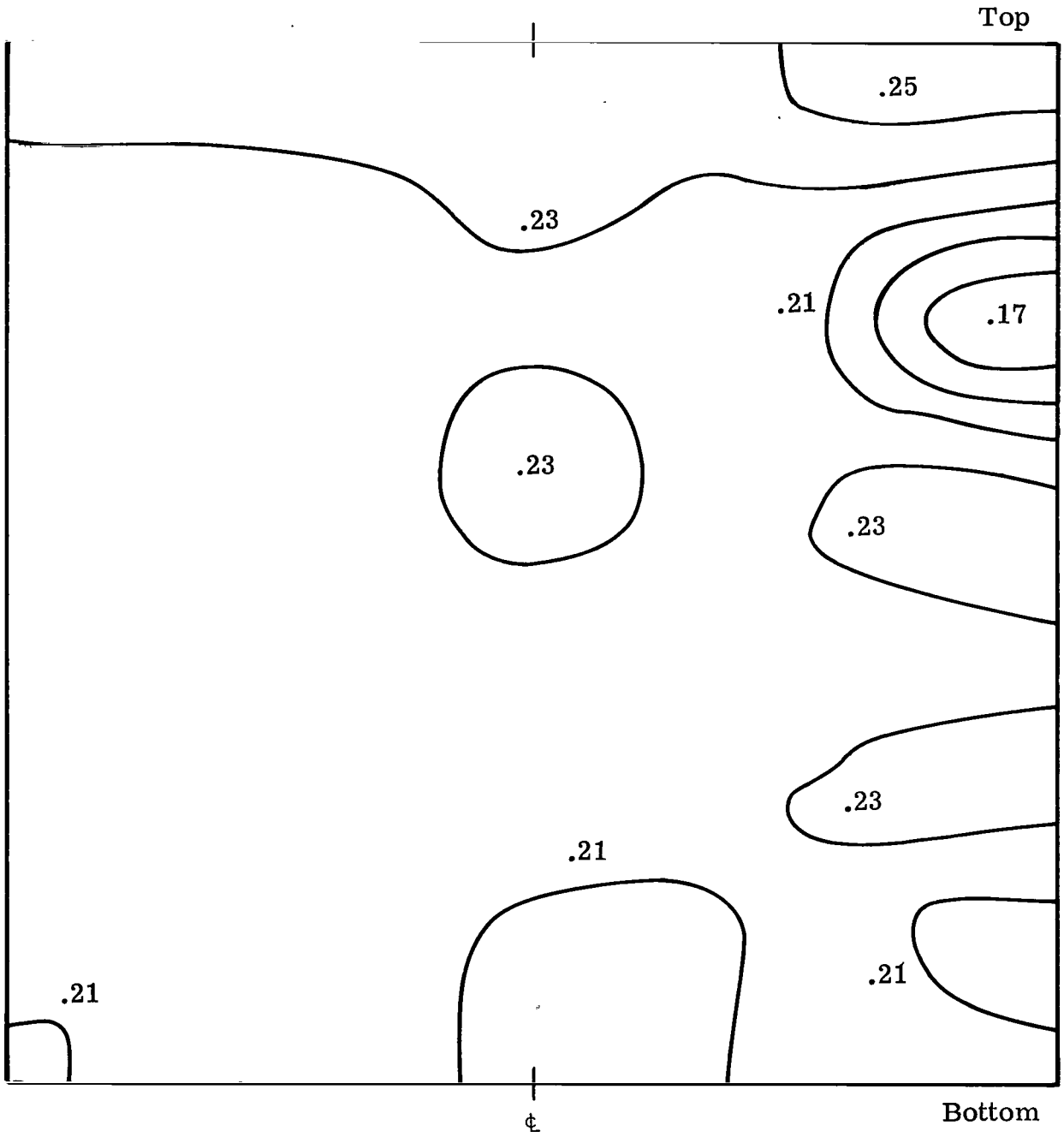

(c) Pitot pressure.

Figure 9.- Continued.

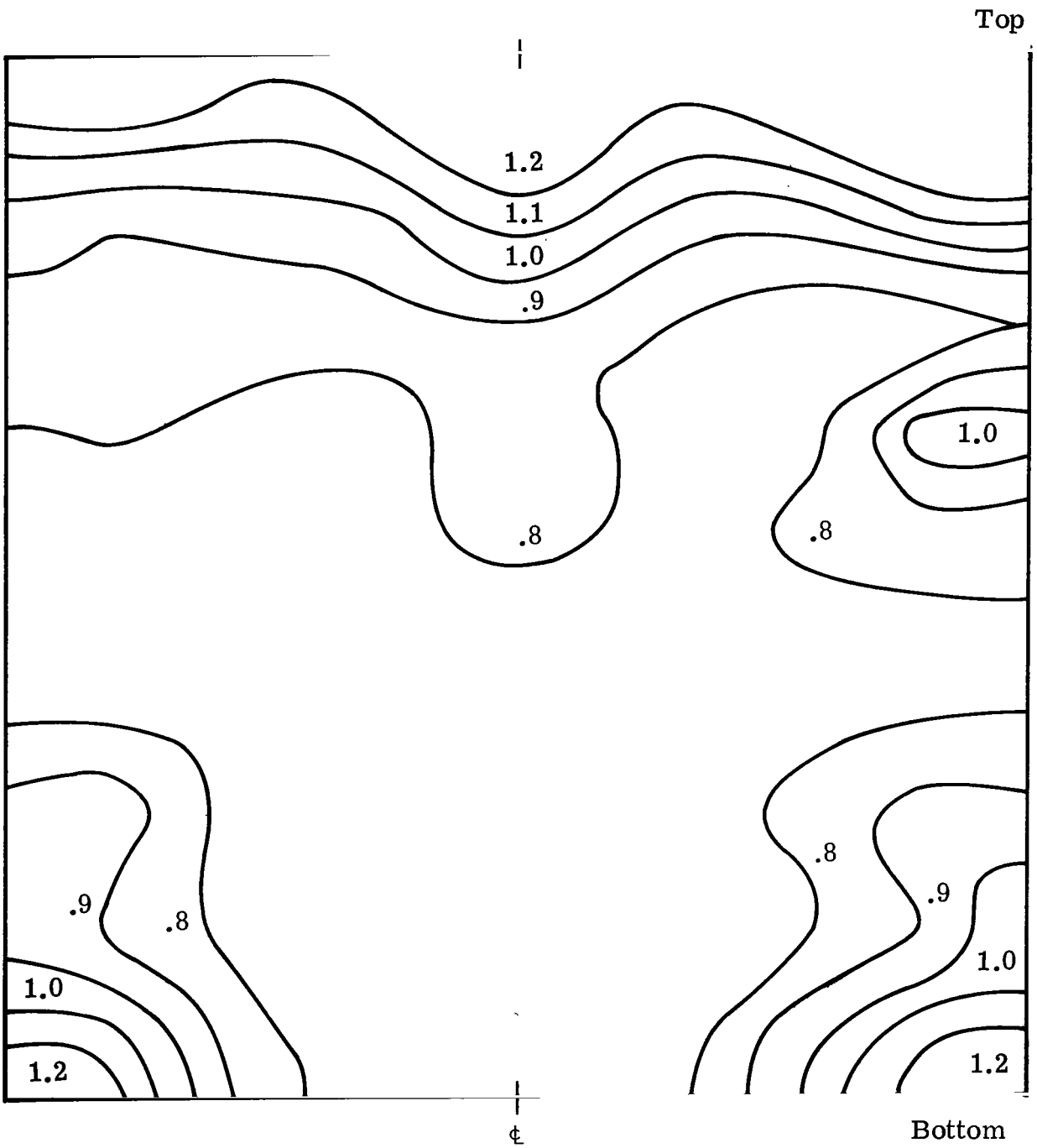

(d) Mass flux.

Figure 9.- Continued.

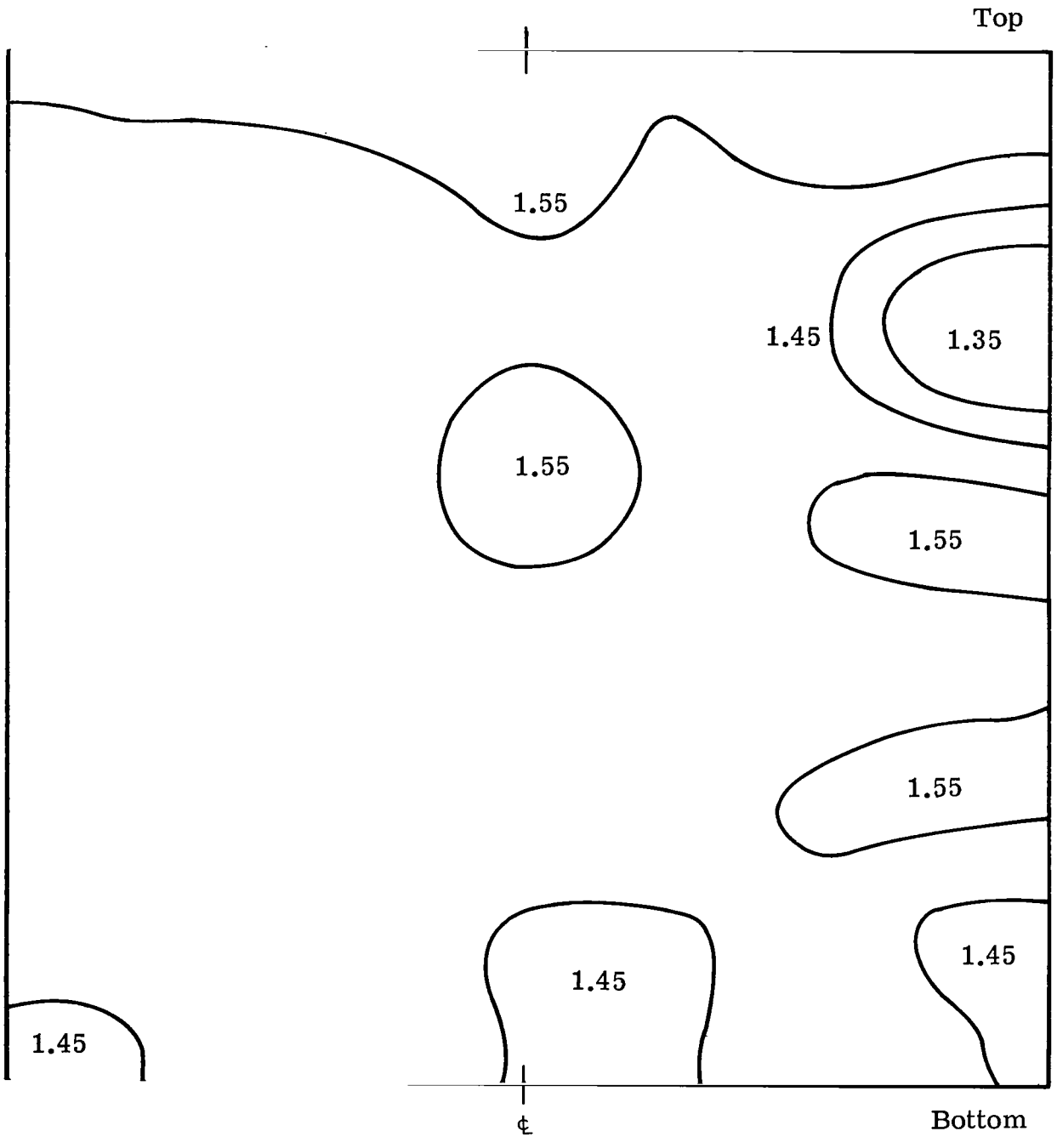

(e) Mach number.

Figure 9.- Continued.

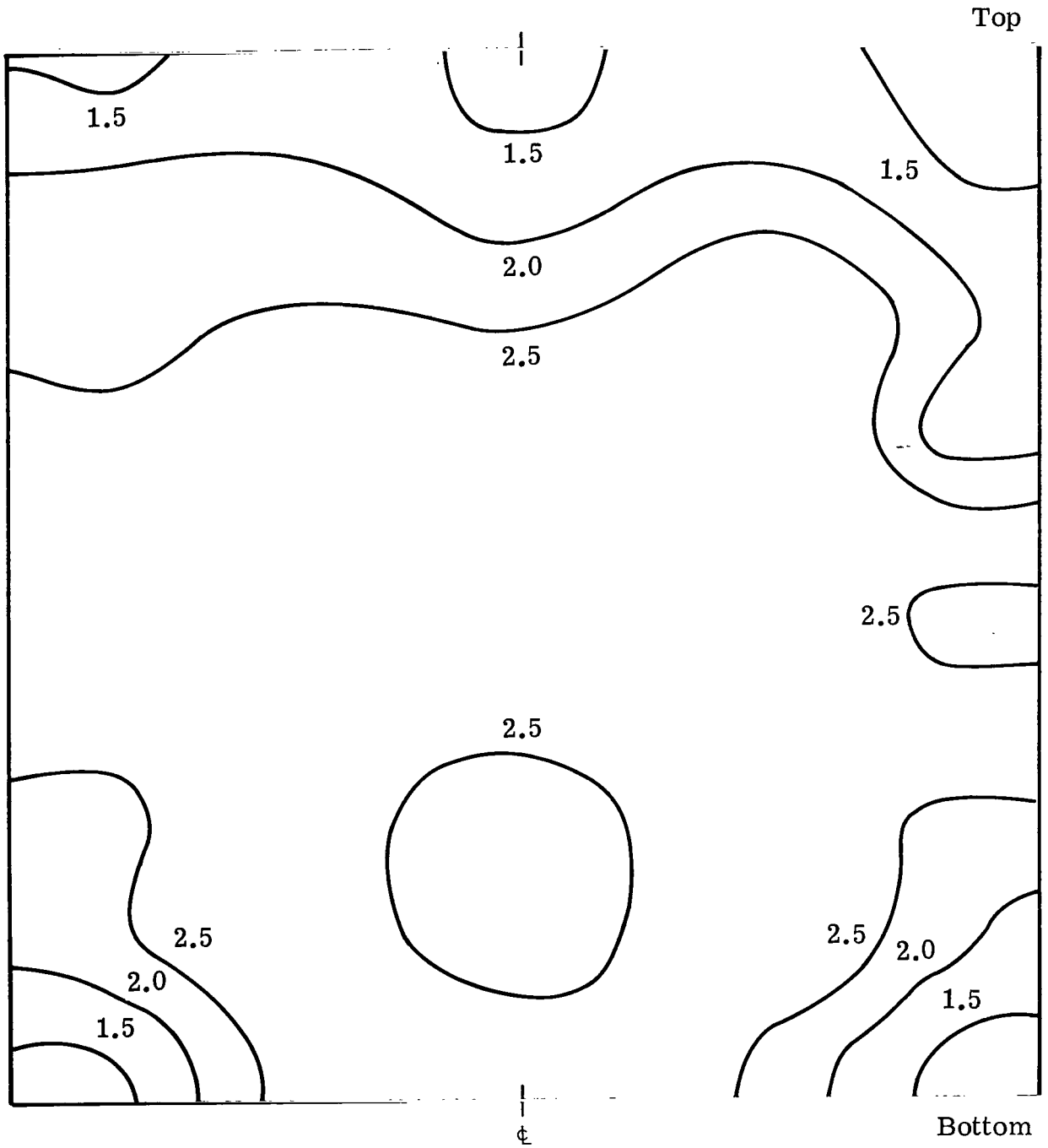

(f) Stagnation temperature.

Figure 9.- Concluded.

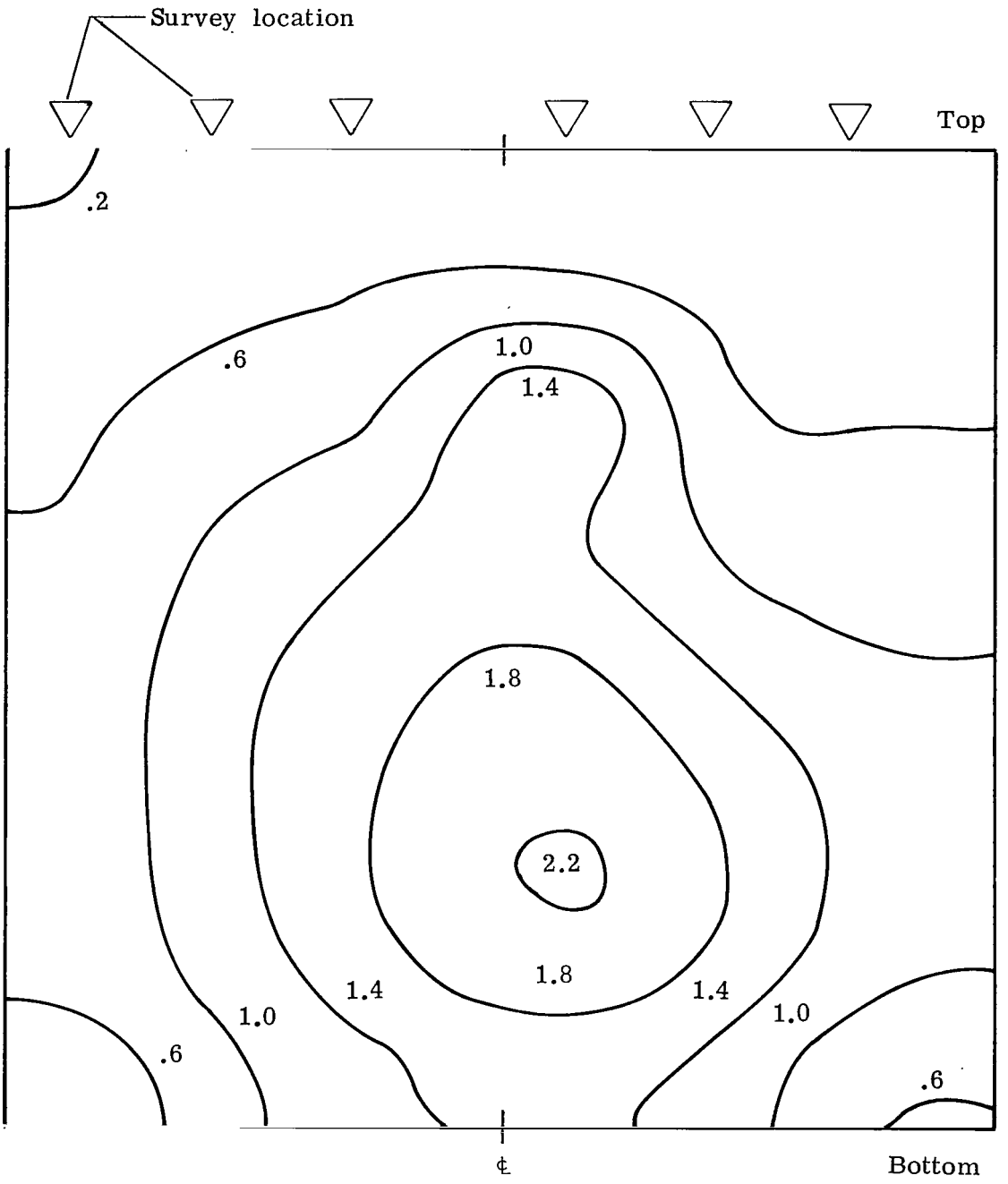

(a) Fuel distribution.

Figure 10.- Surveys of the exit plane of the combustor duct for Mach 1.3 nozzle contour; $\bar{\phi} = 1$.

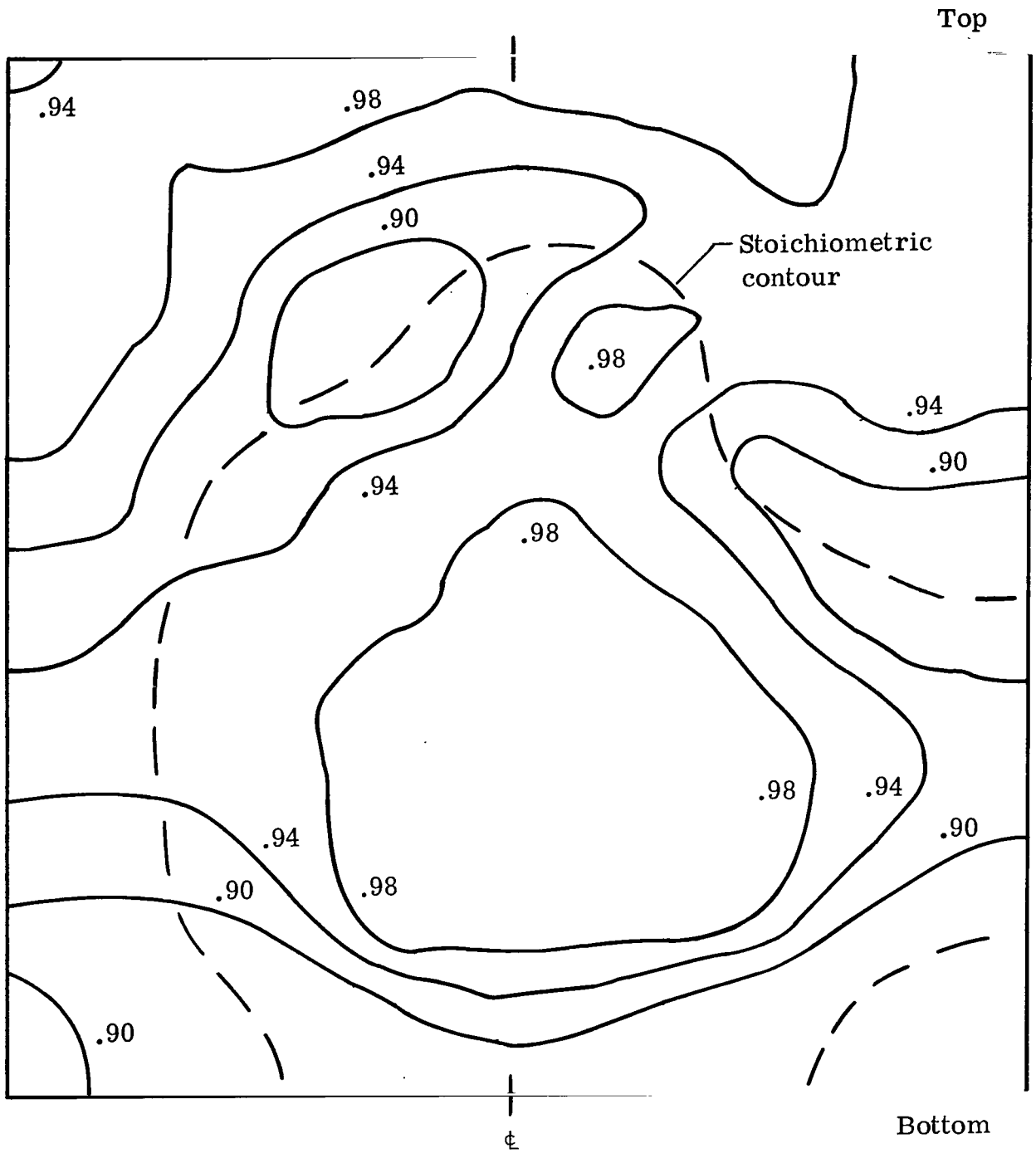

(b) Reaction distribution.

Figure 10.- Continued.

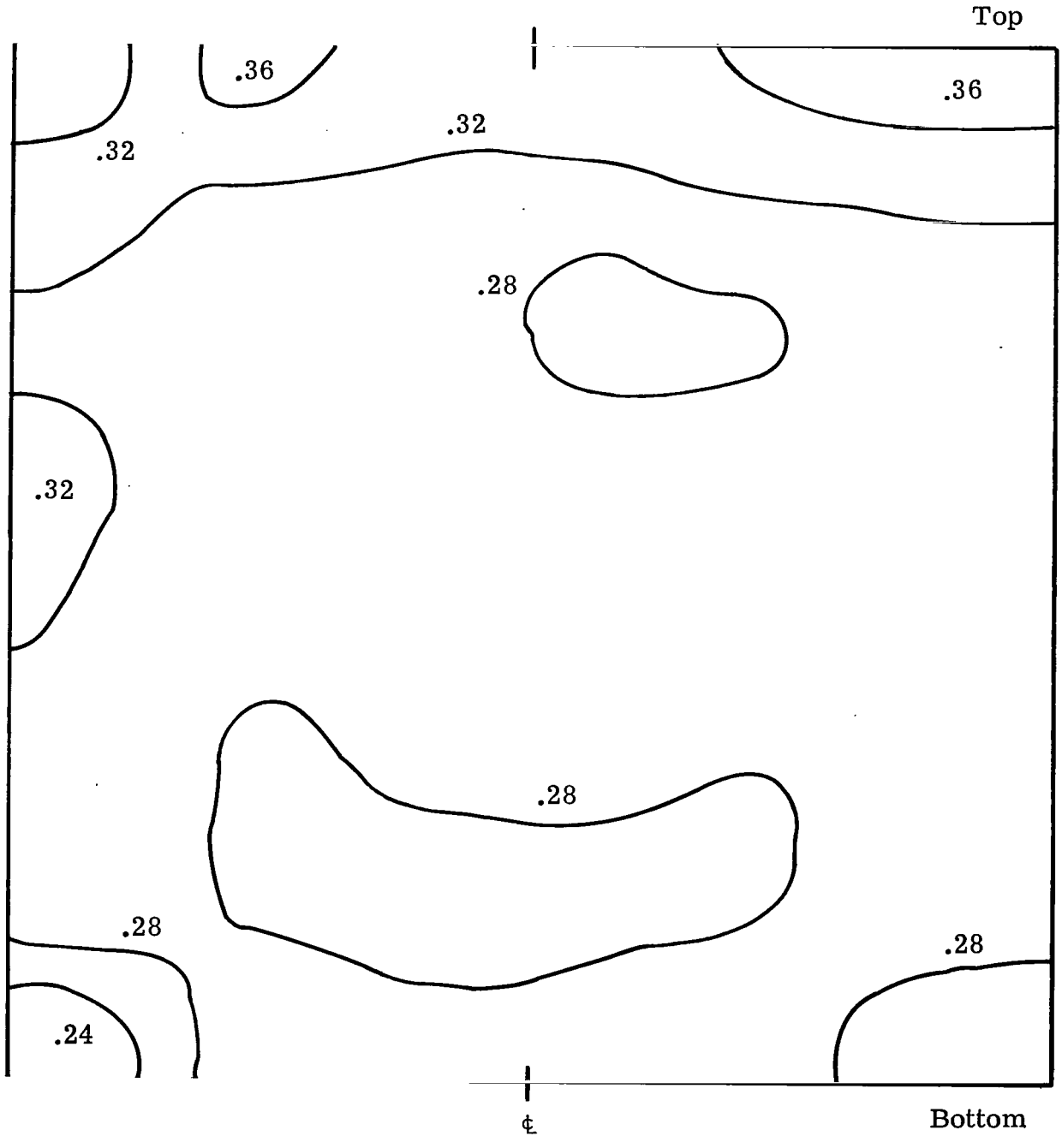

(c) Pitot pressure.

Figure 10.- Continued.

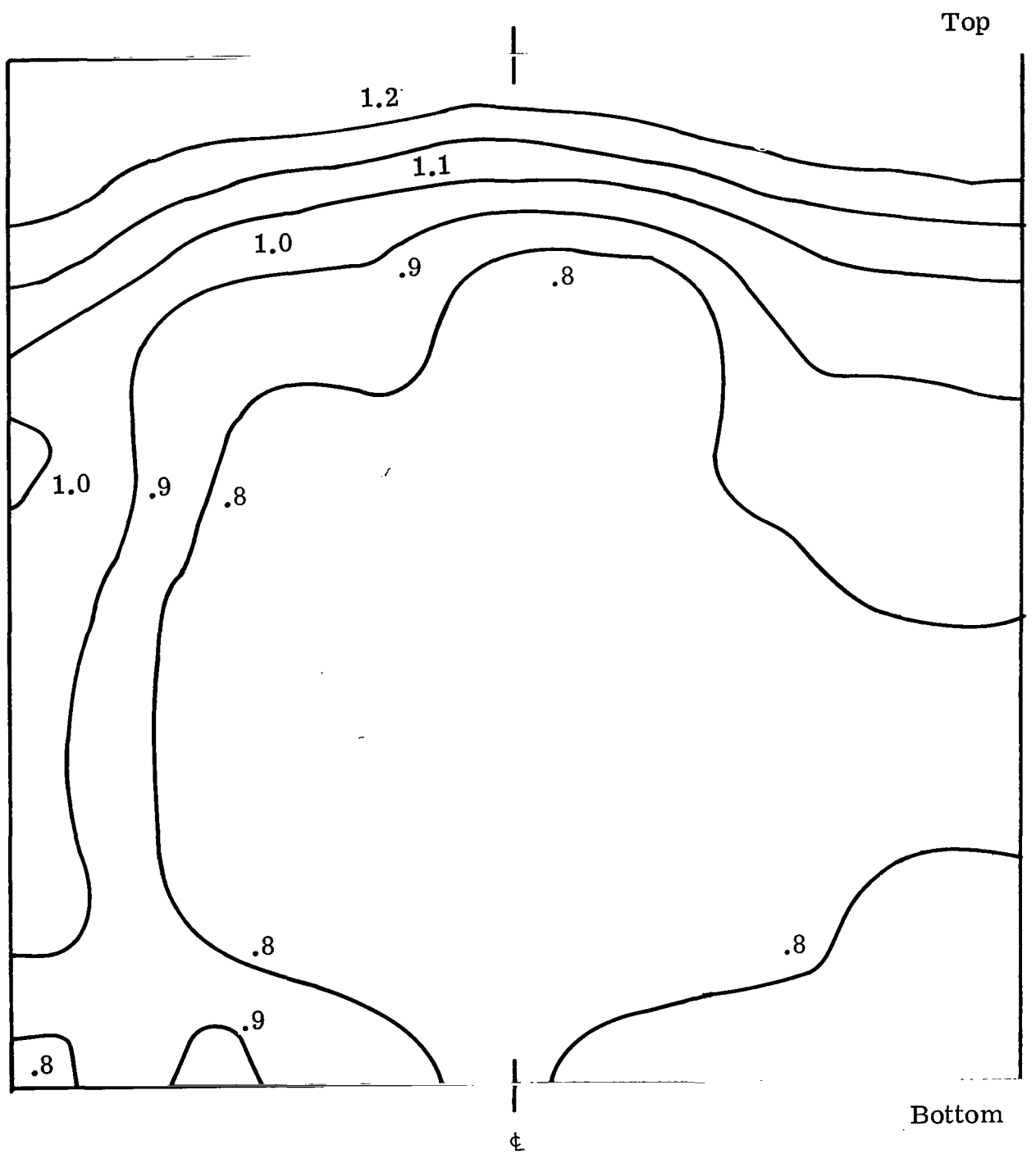

(d) Mass flux.

Figure 10.- Continued.

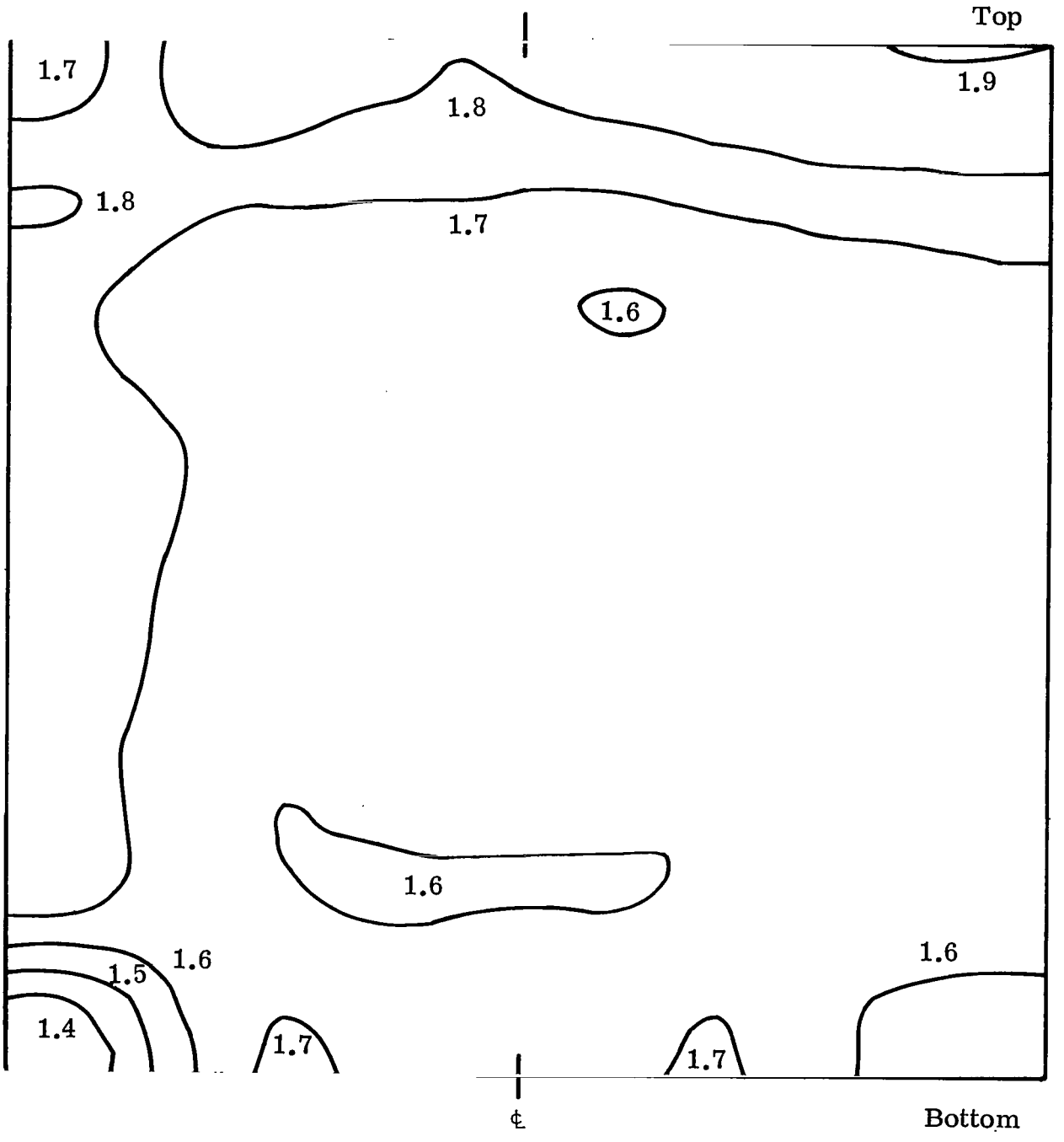

(e) Mach number.

Figure 10.- Continued.

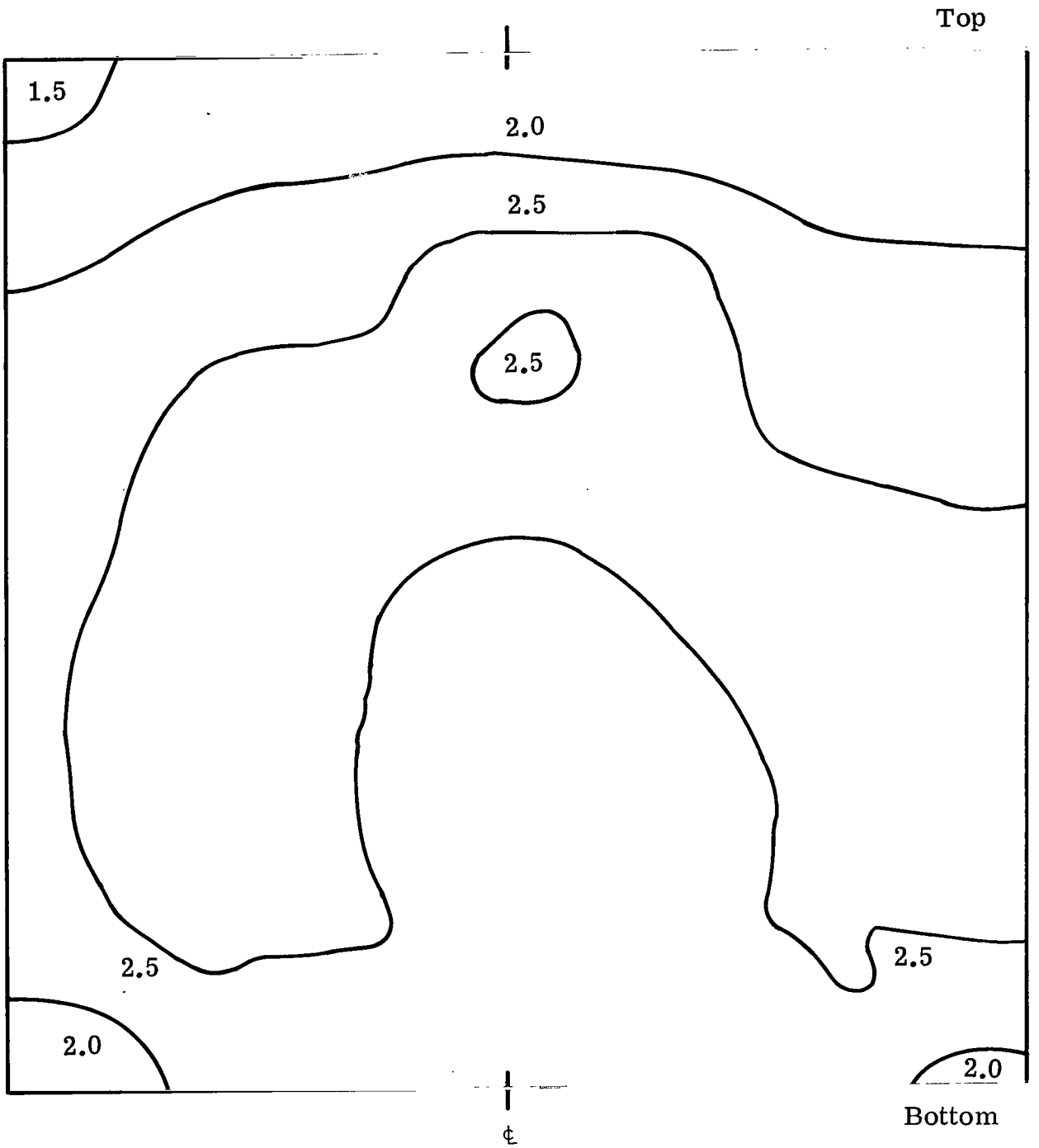

(f) Stagnation temperature.

Figure 10.- Concluded.

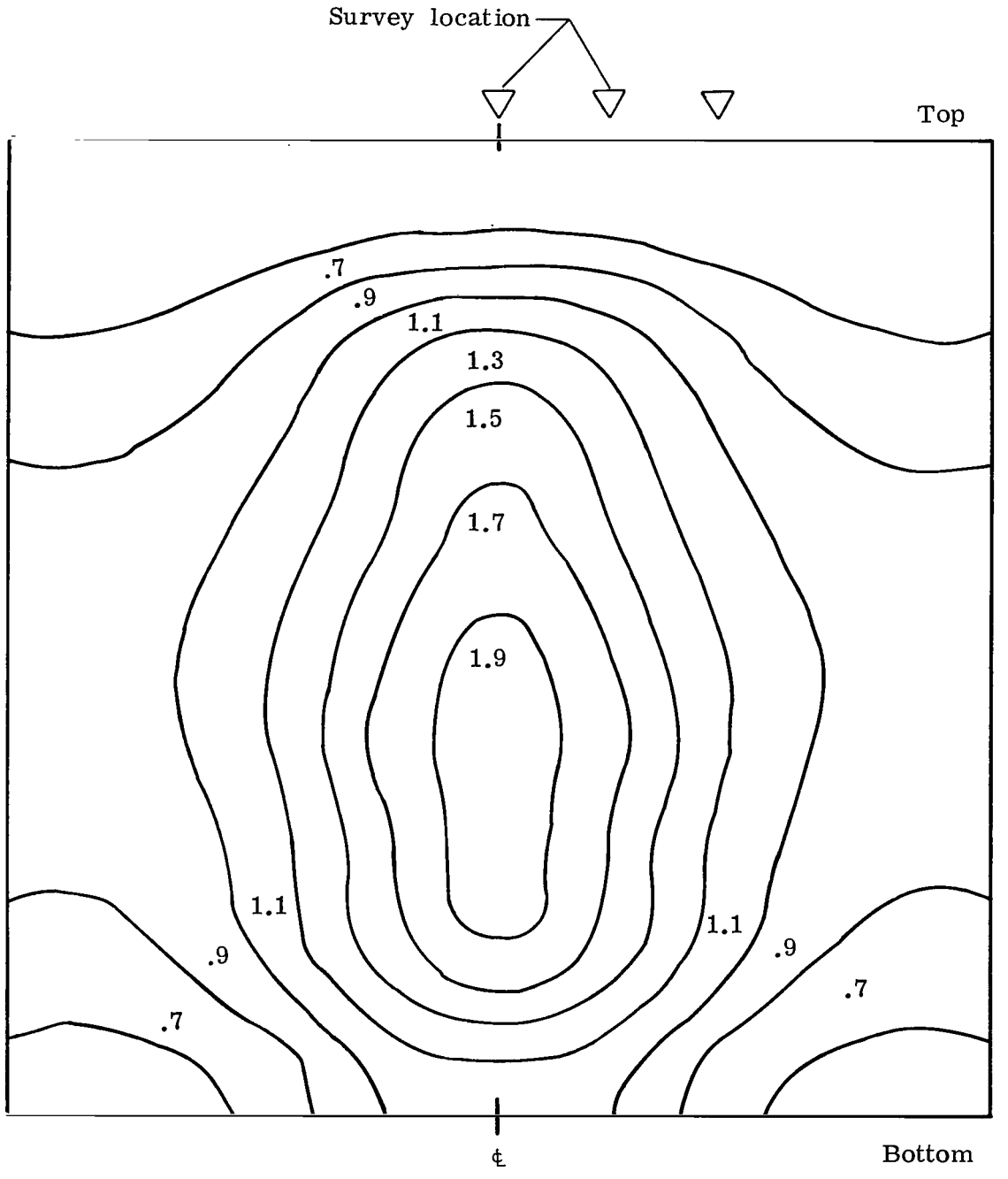

(a) Fuel distribution.

Figure 11.- Surveys of the exit plane of the combustor duct for Mach 1.3 nozzle contour with 450 K heated fuel supplied to perpendicular injectors; $\bar{\phi}$ = 1.

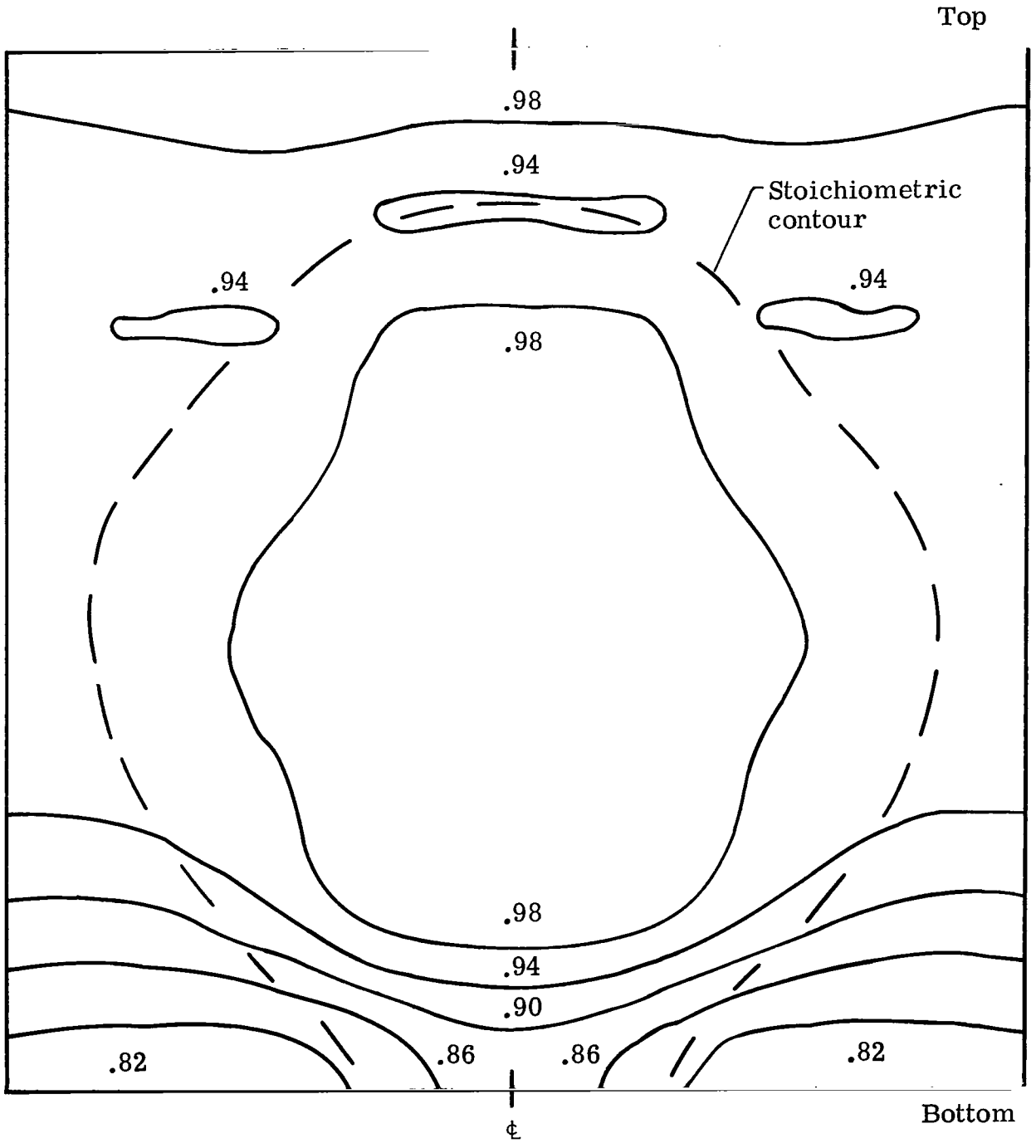

(b) Reaction distribution.

Figure 11.- Continued.

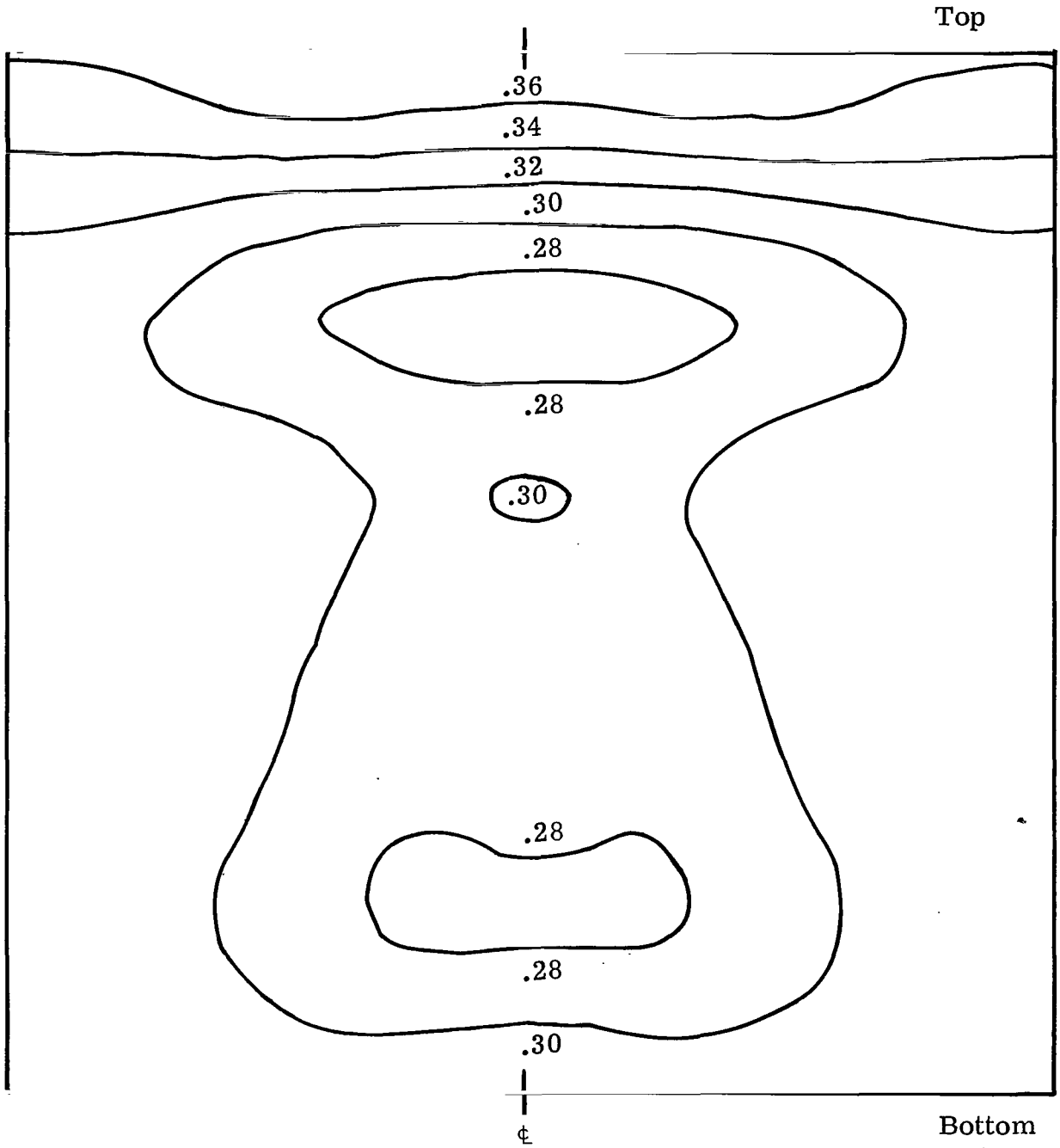

(c) Pitot pressure.

Figure 11.- Continued.

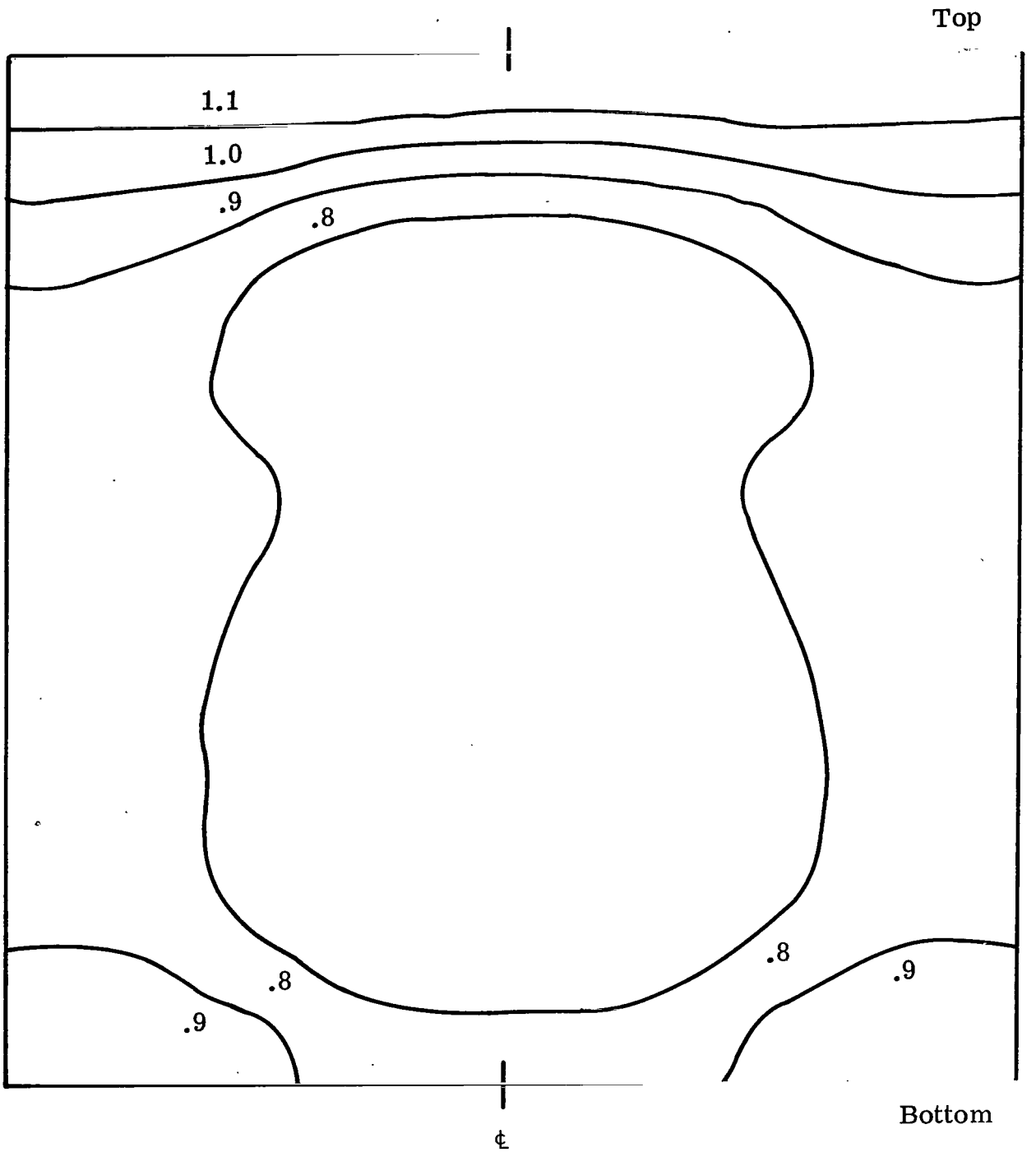

(d) Mass flux.

Figure 11.- Continued.

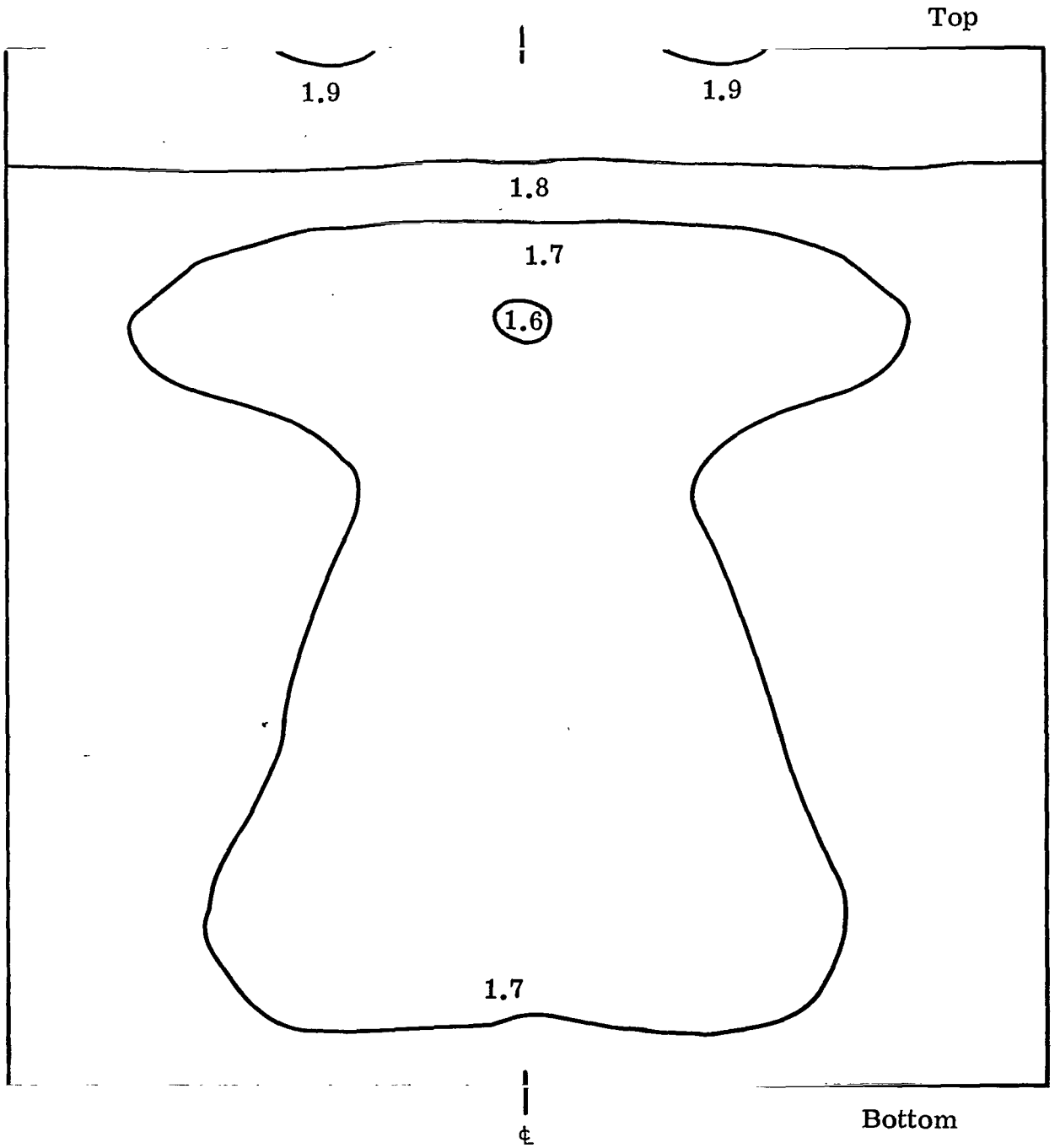

(e) Mach number.

Figure 11.- Continued.

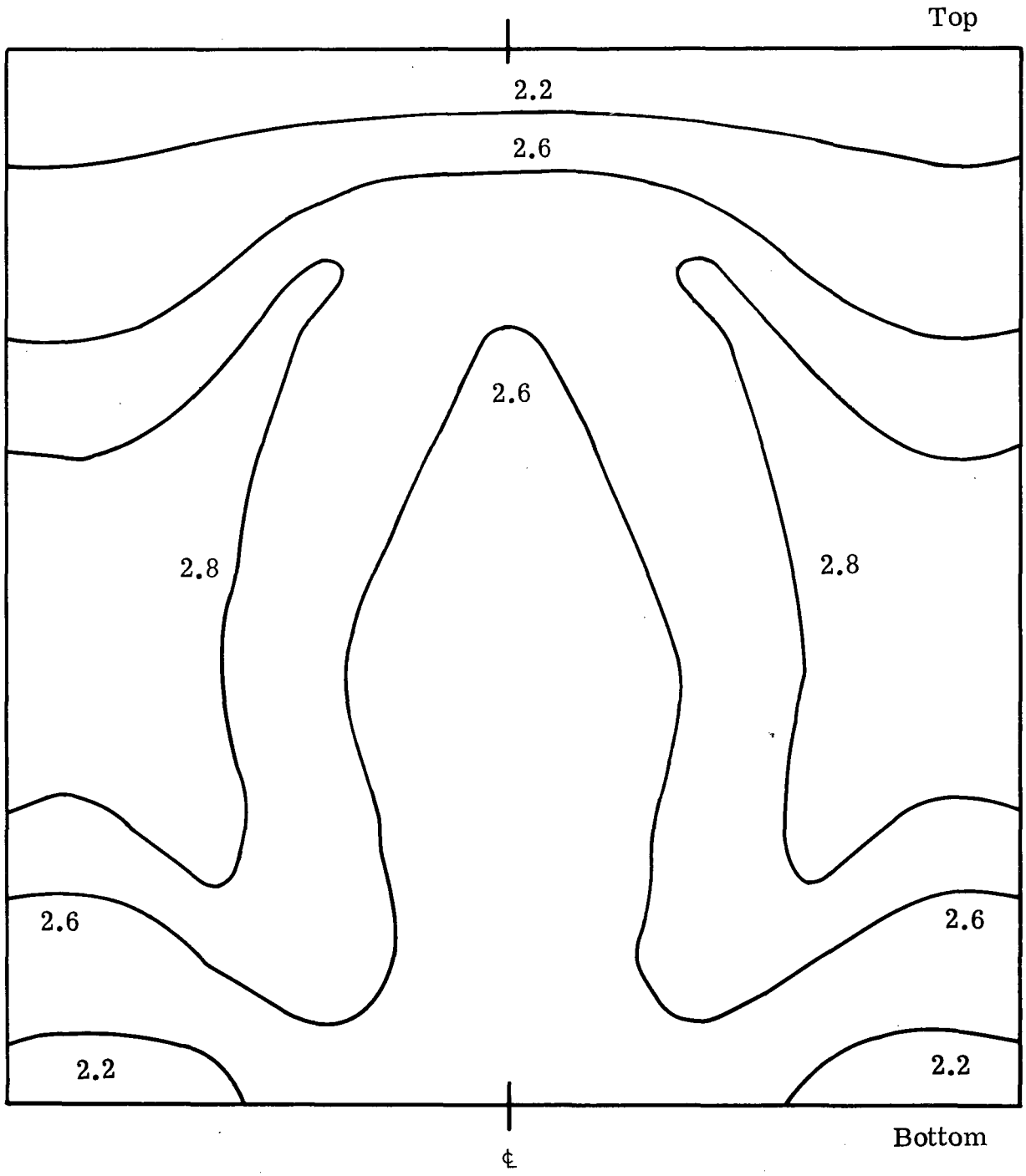

(f) Stagnation temperature.

Figure 11.- Concluded.

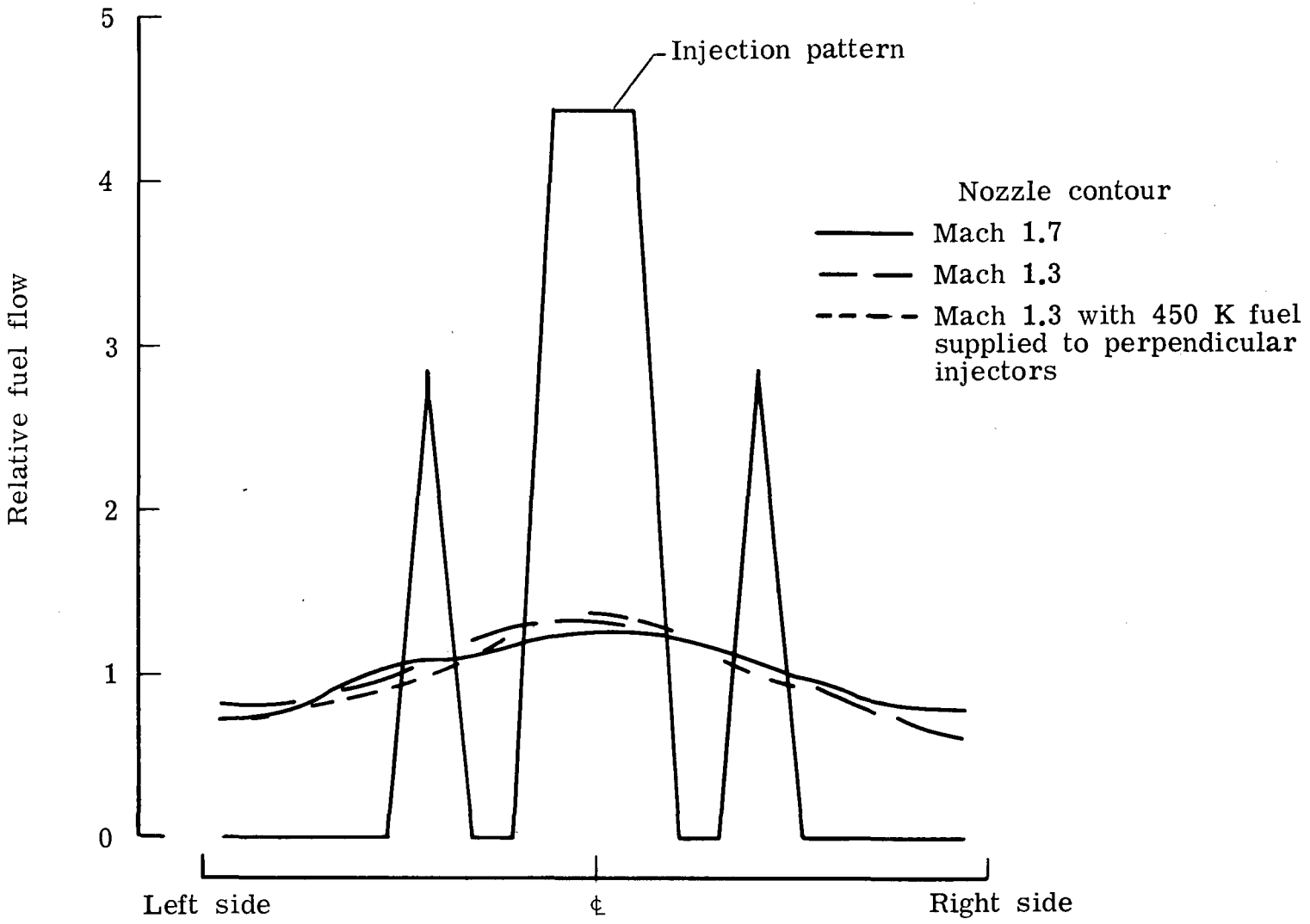

(a) Horizontal fuel distribution.

Figure 12.- Strip integrations.

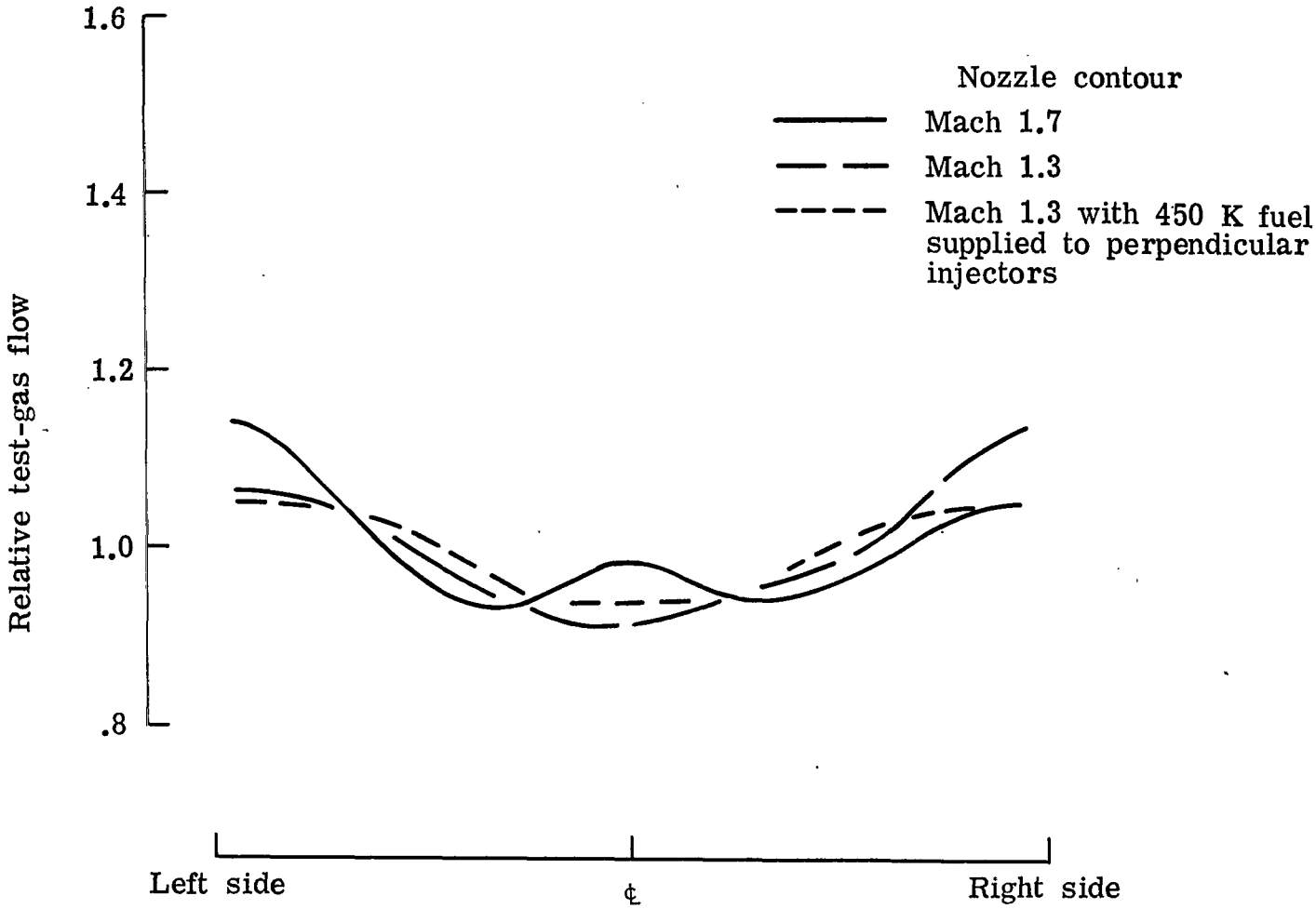

(b) Horizontal test-gas distribution.

Figure 12.- Continued.

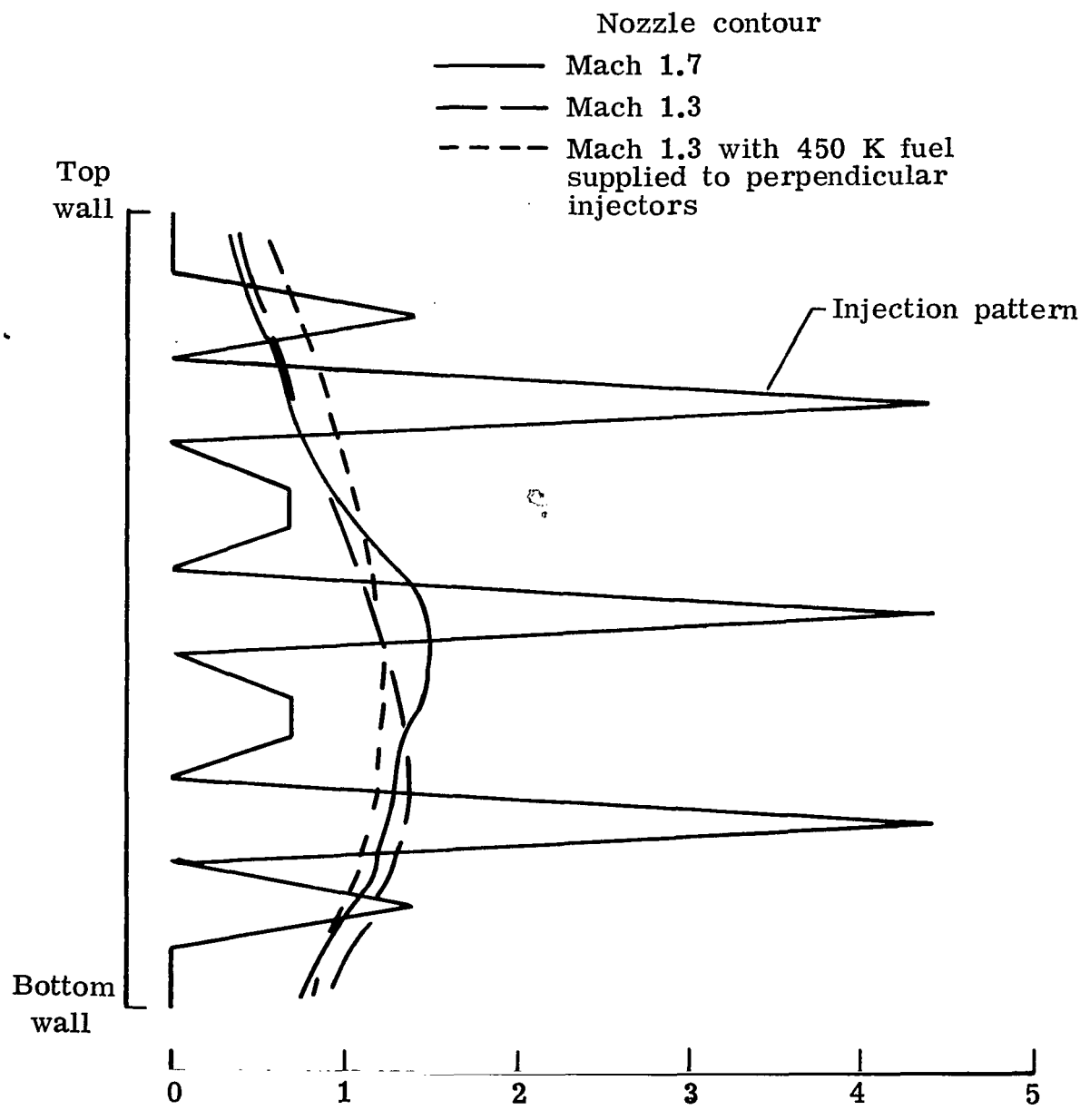

(c) Vertical fuel distribution.

Figure 12.- Continued.

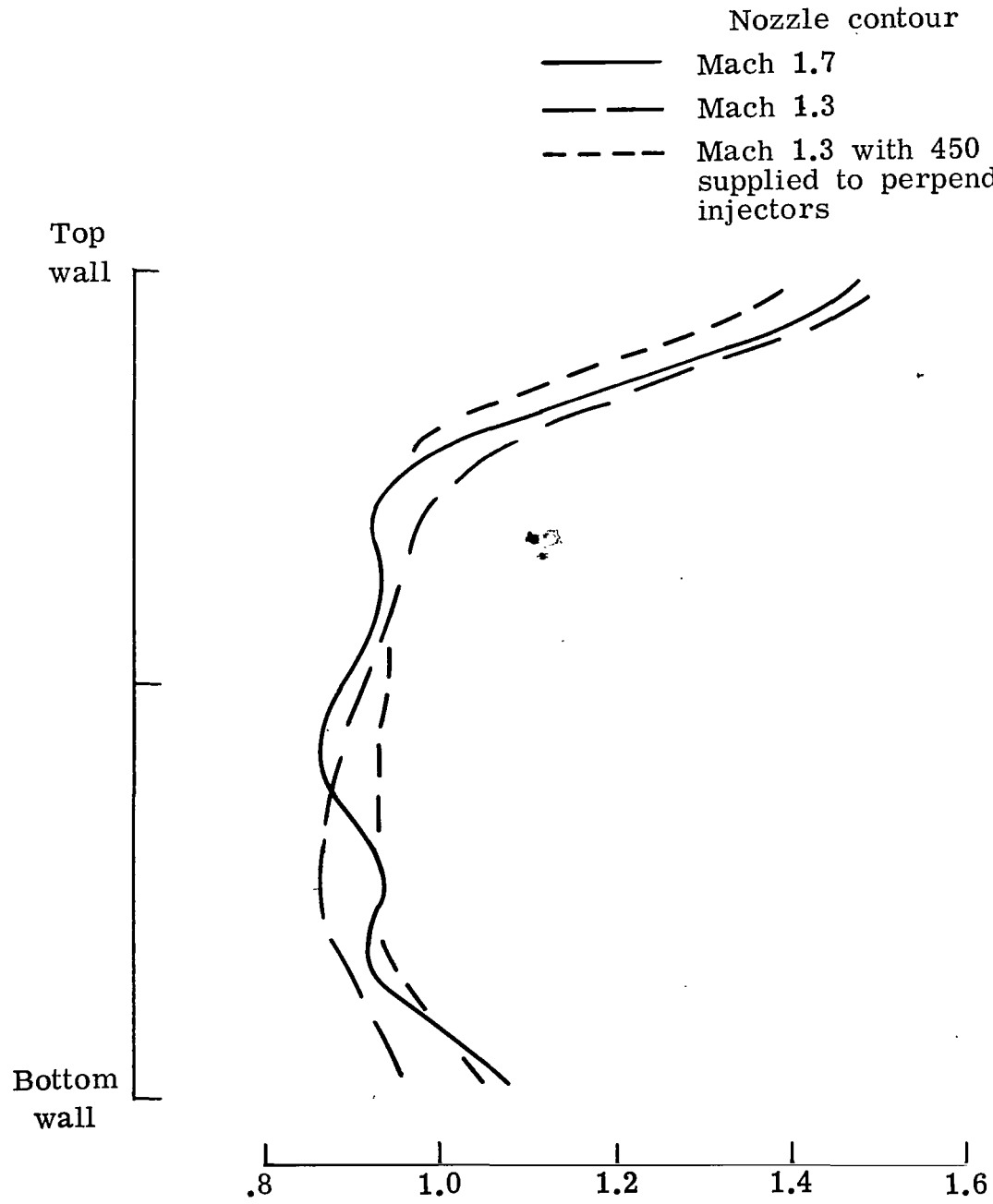

(d) Vertical test-gas distribution.

Figure 12.- Concluded.

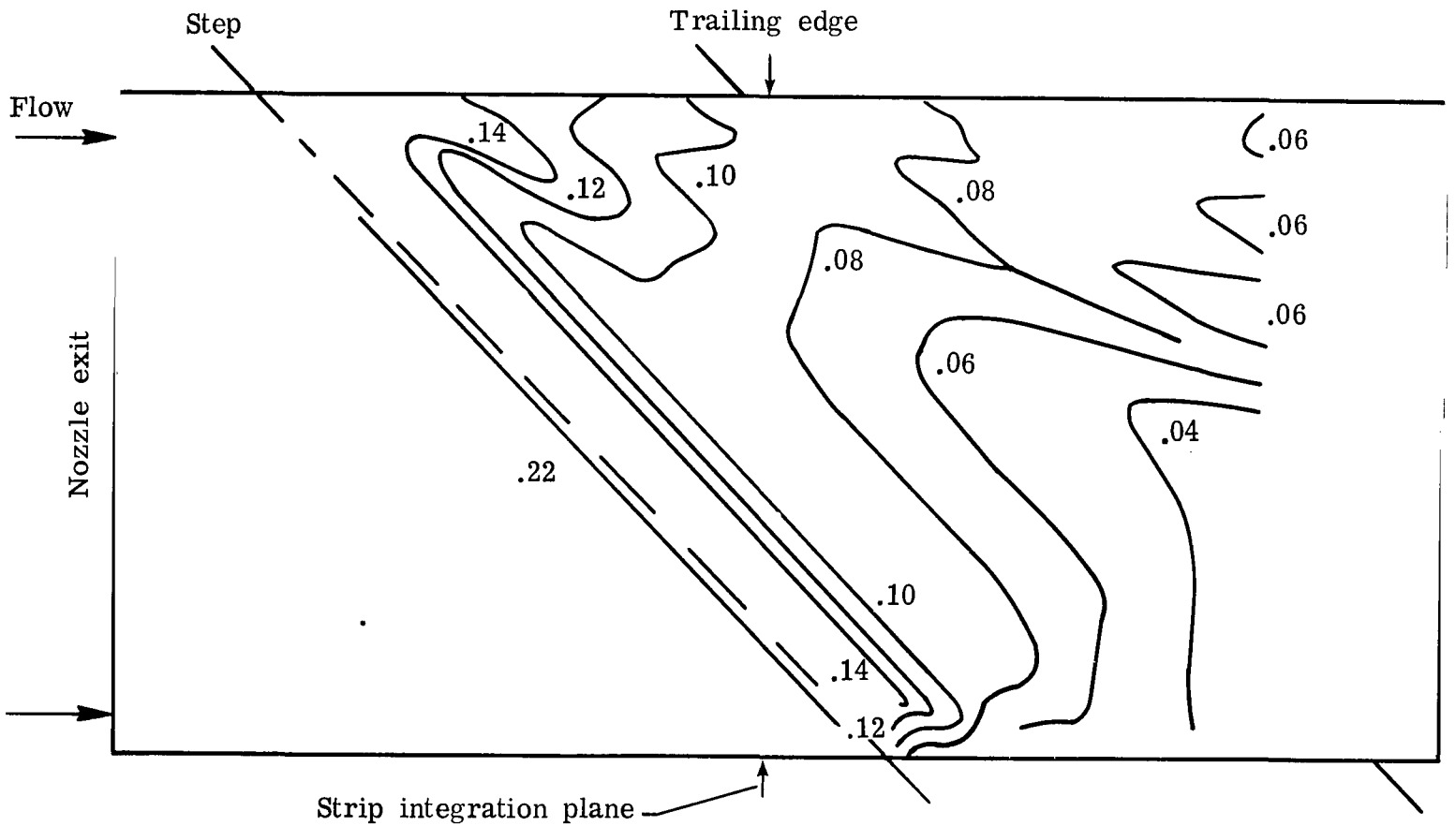

(a) Isobars in swept injector section for Mach 1.7 nozzle contour.

Figure 13.- Calculated flow with no fuel injection.

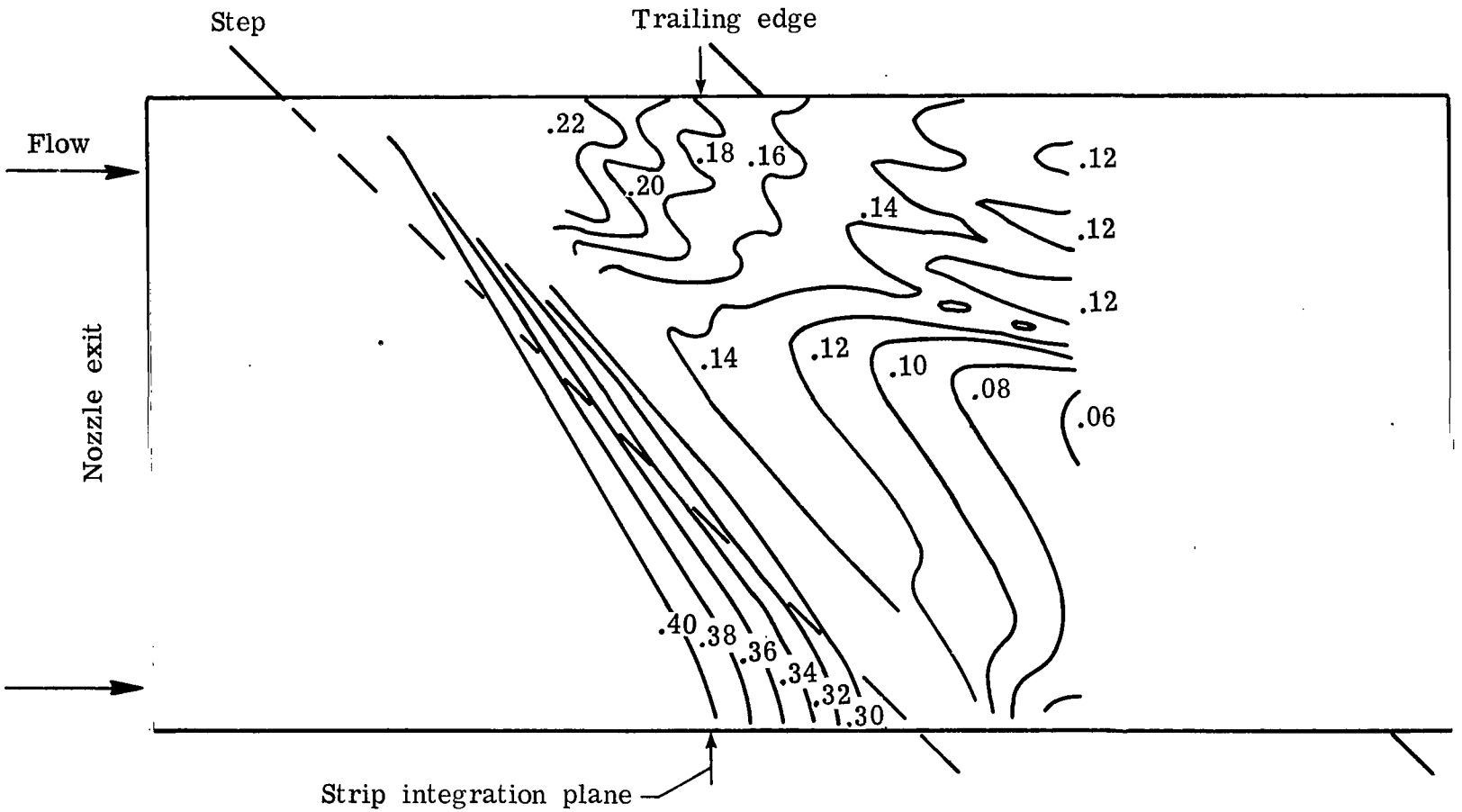

(b) Isobars in swept injector section for Mach 1.3 nozzle contour.

Figure 13.- Continued.

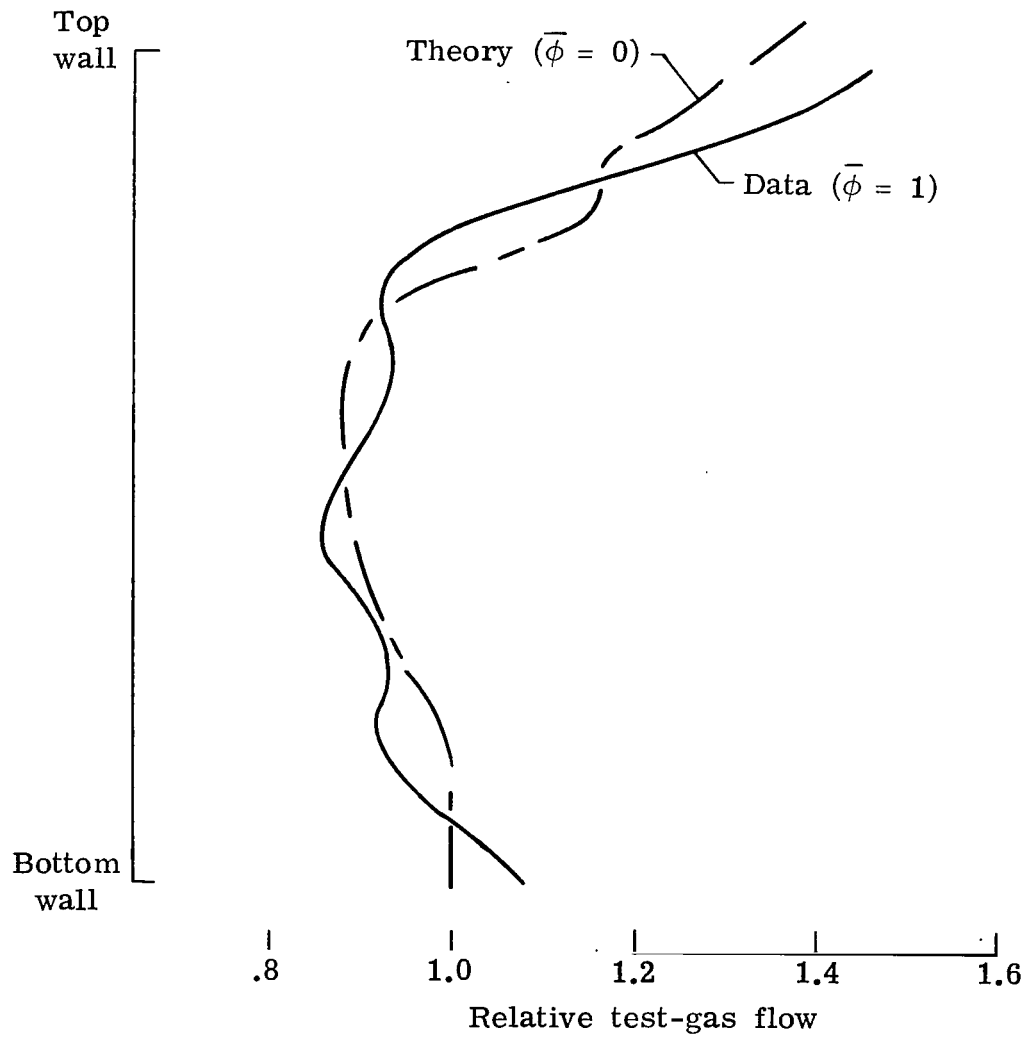

(c) Comparison of vertical test-gas distributions for Mach 1.7 nozzle contour.

Figure 13.- Continued.

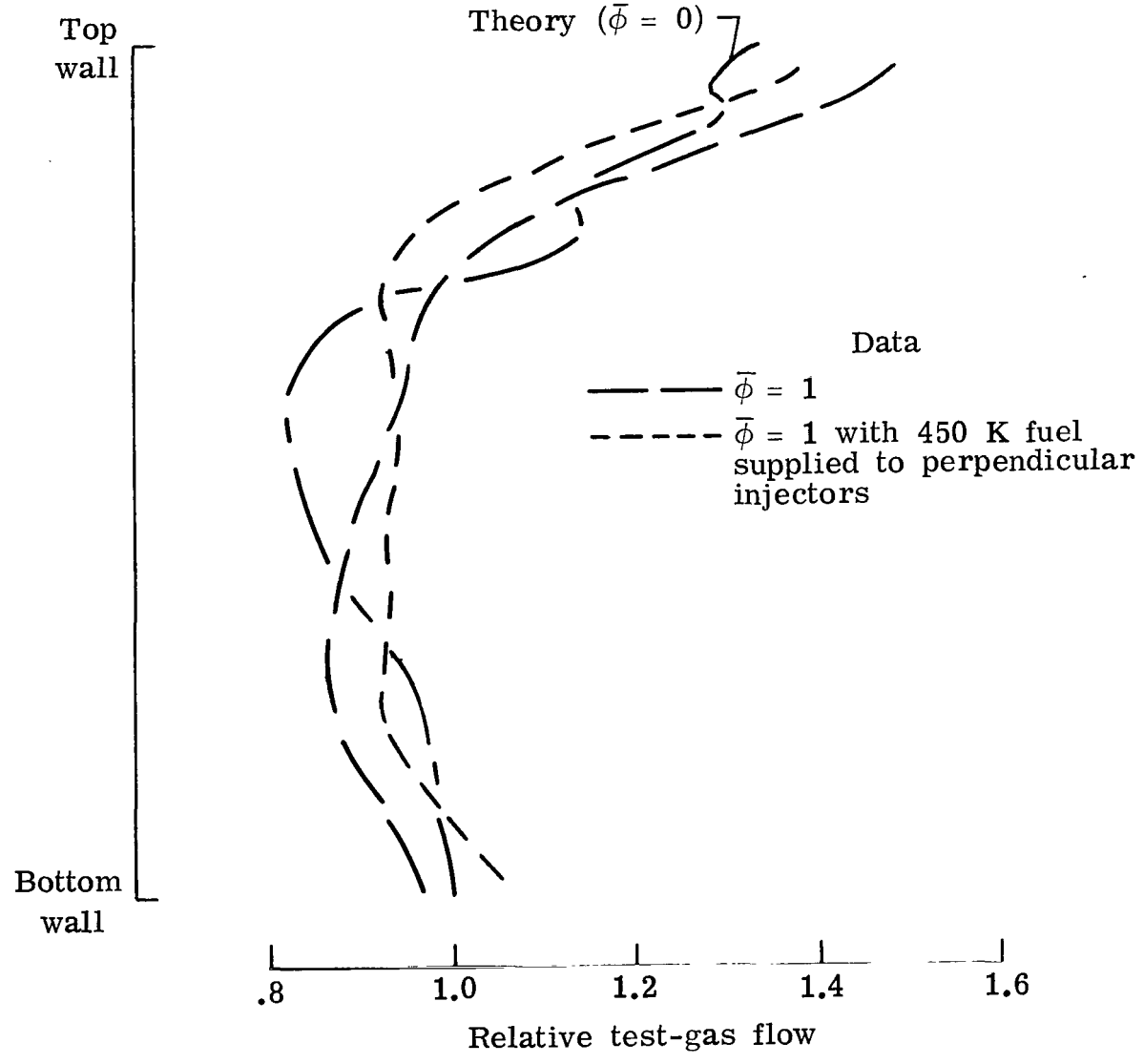

(d) Comparison of vertical test-gas distributions for Mach 1.3 nozzle contour.

Figure 13.- Concluded.

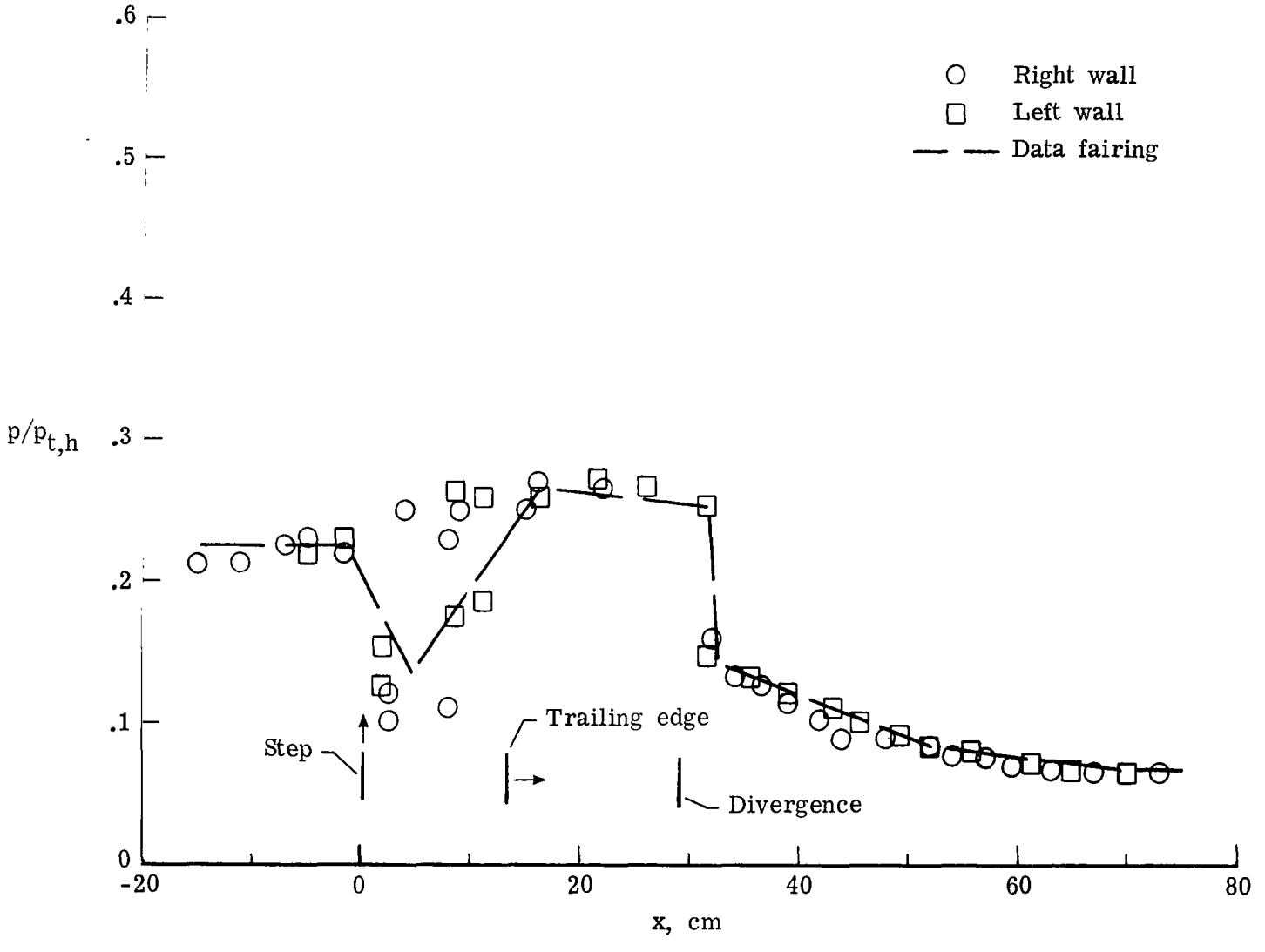

(a) Mach 1.7 nozzle contour.

Figure 14.- Axial wall pressure distribution.

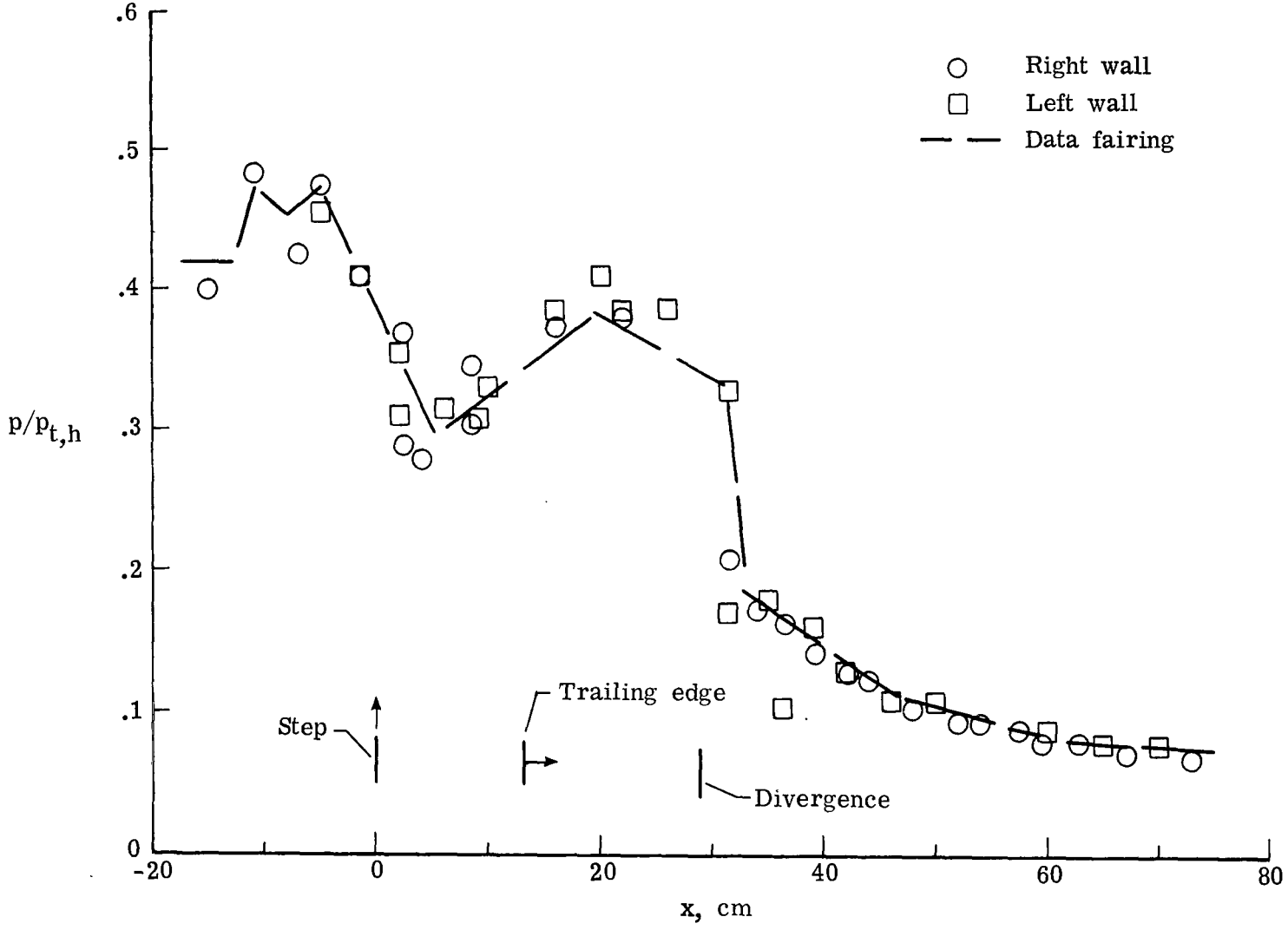

(b) Mach 1.3 nozzle contour.

Figure 14.- Concluded.

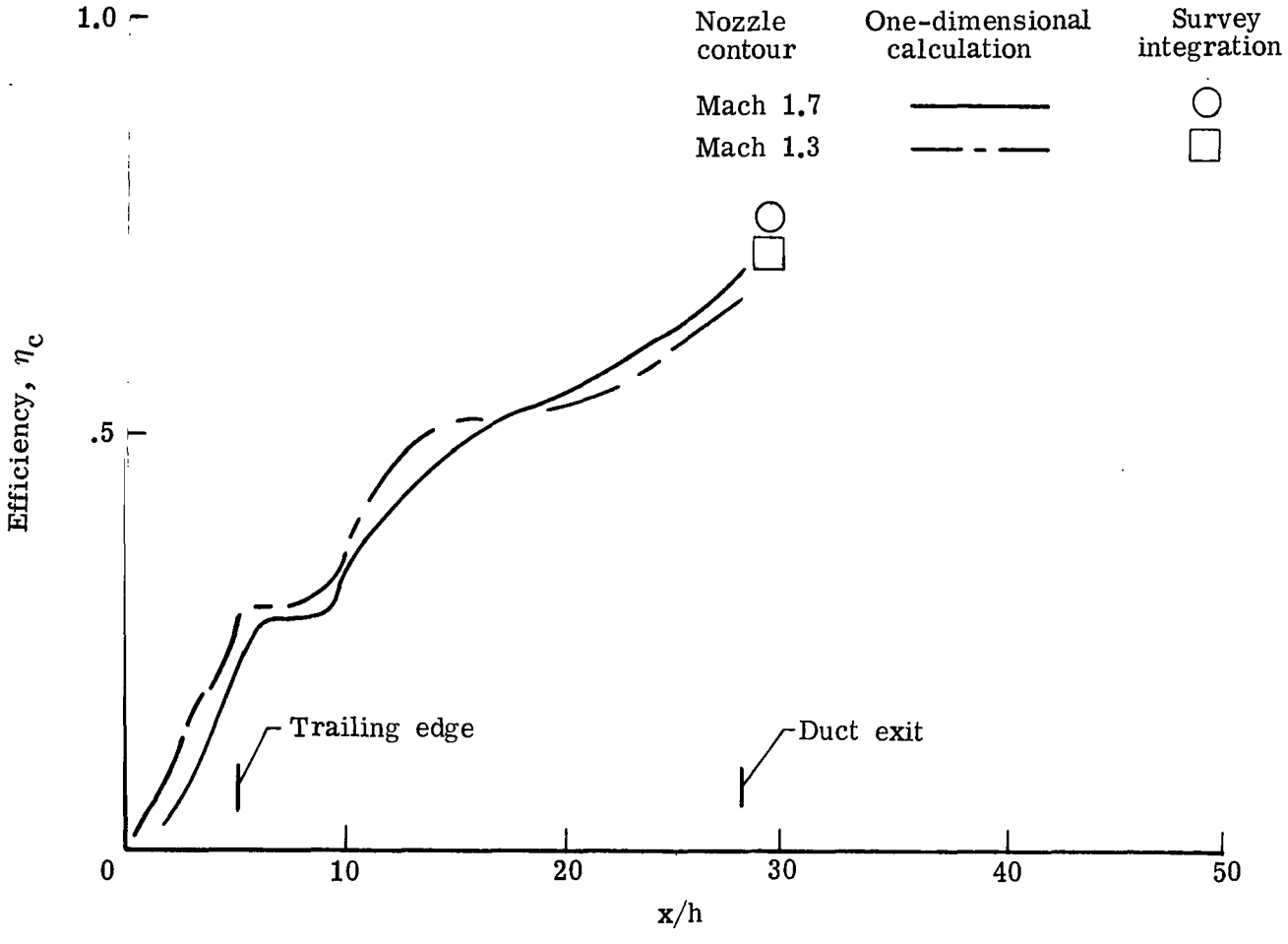

Figure 15.- Axial combustion efficiency distribution.

"The aeronautical and space activities of the United States shall be conducted so as to contribute . . . to the expansion of human knowledge of phenomena in the atmosphere and space. The Administration shall provide for the widest practicable and appropriate dissemination of information concerning its activities and the results thereof."

—NATIONAL AERONAUTICS AND SPACE ACT OF 1958

NASA SCIENTIFIC AND TECHNICAL PUBLICATIONS

TECHNICAL REPORTS: Scientific and technical information considered important, complete, and a lasting contribution to existing knowledge.

TECHNICAL NOTES: Information less broad in scope but nevertheless of importance as a contribution to existing knowledge.

TECHNICAL MEMORANDUMS: Information receiving limited distribution because of preliminary data, security classification, or other reasons. Also includes conference proceedings with either limited or unlimited distribution.

CONTRACTOR REPORTS: Scientific and technical information generated under a NASA contract or grant and considered an important contribution to existing knowledge.

TECHNICAL TRANSLATIONS: Information published in a foreign language considered to merit NASA distribution in English.

SPECIAL PUBLICATIONS: Information derived from or of value to NASA activities. Publications include final reports of major projects, monographs, data compilations, handbooks, sourcebooks, and special bibliographies.

TECHNOLOGY UTILIZATION PUBLICATIONS: Information on technology used by NASA that may be of particular interest in commercial and other non-aerospace applications. Publications include Tech Briefs, Technology Utilization Reports and Technology Surveys.

Details on the availability of these publications may be obtained from:

SCIENTIFIC AND TECHNICAL INFORMATION OFFICE

NATIONAL AERONAUTICS AND SPACE ADMINISTRATION

Washington, D.C. 20546